



Spectrochemical determination of unique bacterial responses following long-term low-level exposure to antimicrobials

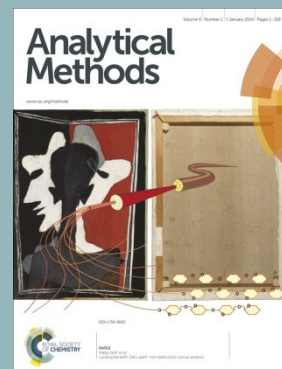
Journal:	<i>Analytical Methods</i>
Manuscript ID	AY-ART-01-2018-000011.R1
Article Type:	Paper
Date Submitted by the Author:	n/a
Complete List of Authors:	Jin, Naifu; Lancaster University, Lancaster Environment Centre Semple, Kirk; Lancaster University, Dept of Environmental Science Jiang, Longfei; Guangzhou Institute of Geochemistry, Analytical Chemistry Luo, Chunling; Guangzhou Institute of Geochemistry, Chinese Academy of Sciences, Martin, Francis; University of Central Lancashire, School of Pharmacy and Biomedical Sciences; Lancaster University, Centre for Biophotonics Zhang, Dayi; Lancaster University,

Analytical Methods – Guidelines for Reviewers

Analytical Methods publishes research detailing early applied demonstrations of new analytical methods which address key issues of societal concern.

When considering manuscripts for publication in *Analytical Methods*, please consider:

1. Manuscripts must be of good quality with high scientific integrity
2. Routine and incremental work – however competently researched and reported – should not be recommended for publication
3. Papers should be accompanied by a statement of societal impact
4. Sister journal *Analyst* publishes work on premier fundamental discoveries, inventions and applications in the analytical and bioanalytical sciences. See more information [here](#).



Thank you very much for your assistance in evaluating this manuscript

General Guidance

Journal Scope: Details regarding the scope of *Analytical Methods* (including example topics covered) can be found [here](#).

Reviewers have the responsibility to treat the manuscript as confidential. Please be aware of our [Ethical Guidelines](#), which contain full information on the responsibilities of reviewers and authors, and our [Refereeing Procedure and Policy](#).

It is essential that all articles submitted to *Analytical Methods* meet the significant novelty criteria;

Lack of novelty is sufficient reason for rejection.

When preparing your report, please:

- Comment on the originality, significance, impact and scientific reliability of the work;
- State clearly whether you would like to see the article accepted or rejected and give detailed comments (with references, as appropriate) that will both help the Editor to make a decision on the article and the authors to improve it.

Please inform the Editor if:

- There is a conflict of interest;
- There is a significant part of the work which you are not able to referee with confidence;
- The work, or a significant part of the work, has previously been published;
- You believe the work, or a significant part of the work, is currently submitted elsewhere;
- The work represents part of an unduly fragmented investigation.

Submit your report at

<http://mc.manuscriptcentral.com/ay>

For further information about *Analytical Methods* please visit: <http://www.rsc.org/methods>

If you have any questions about reviewing this manuscript please contact the Editorial Office: methods@rsc.org

Statement of Societal Impact

The majority of laboratory studies examining bacterial responses to antimicrobial agents have been in typical laboratory nutrient-rich and short-exposure culture scenarios. How this translates to real-world environmental conditions where bacteria inhabit a nutrient-depleted environment and exposures tend to be long-term remains to be examined. This study applied a non-destructive spectrochemical analysis to examine this question. We demonstrate that exposure time is a major confounding factor in bacterial responses to antimicrobials, as has nutrient depletion. This study has major impact in understanding different bacterial responses to real-world exposures to antimicrobials. Given the emerging resistance of bacteria to such agents, this is of enormous significance.

1
2
3 **1 Spectrochemical determination of unique bacterial responses following long-term low-**
4 **2 level exposure to antimicrobials**

5
6
7 3 Naifu Jin^{a,b}, Kirk T Semple^a, Longfei Jiang^c, Chunling Luo^c, Francis L Martin^{d,*}, Dayi
8 4 Zhang^{a,b,*}
9

10 5 ^a*Lancaster Environment Centre, Lancaster University, Lancaster LA1 4YQ, UK*

11
12
13 6 ^b*School of Environment, Tsinghua University, Beijing 100084, China*

14
15 7 ^c*Guangzhou Institute of Geochemistry, Chinese Academy of Sciences, Guangzhou 510640,*
16 8 *China*

17
18
19 9 ^d*School of Pharmacy and Biomedical Sciences, University of Central Lancashire, Preston*
20 10 *PR1 2HE, UK*
21
22

23
24
25 12 ***Corresponding authors:**

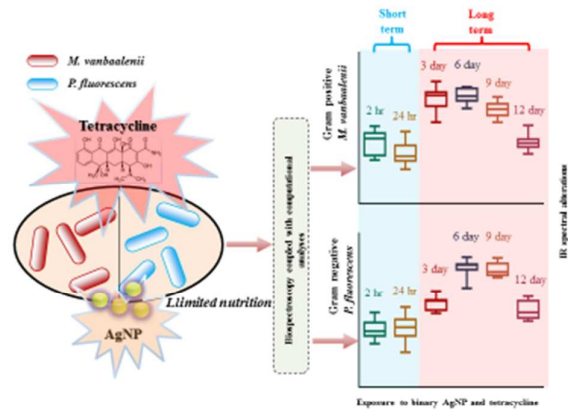
26
27 13 Francis L Martin, School of Pharmacy and Biomedical Sciences, University of Central
28 14 Lancashire, Preston PR1 2HE, UK; Email: flmartin@uclan.ac.uk

29
30
31 15 Dayi Zhang, School of Environment, Tsinghua University, Beijing 100084, China; Email:
32 16 zhangdayi@tsinghua.org.cn
33
34

35 17
36
37
38
39
40
41
42
43
44
45
46
47
48
49
50
51
52
53
54
55
56
57
58
59
60

18 ToC graphic

19



20

21

1
2
3 **22 Abstract**
4

5 23 Agents arising from engineering or pharmaceutical industries may induce significant
6 24 environmental impacts. Particularly, antimicrobials not only act as efficient eliminators of
7 25 certain microbes but also facilitate the propagation of organisms with antimicrobial resistance,
8 26 raising critical health issues, *e.g.*, the bloom of multidrug-resistant bacteria. Although many
9 27 investigations have examined microbial responses to antimicrobials and characterized
10 28 relevant mechanisms, they have focused mainly on high-level and short-term exposures,
11 29 instead of simulating real-world scenarios in which the antimicrobial exposure is at a low-
12 30 level for long periods. Herein, we developed a spectrochemical tool, attenuated total
13 31 reflection Fourier-transform infrared (ATR-FTIR) spectroscopy, as a high-throughput and
14 32 nondestructive approach to interrogate the long-term effects of low-level antimicrobial
15 33 exposure in bacterial cells. Post-exposure to nanoparticulate silver (AgNP), tetracycline or
16 34 their mixtures for 12 days, Gram-positive (*Mycobacterium vanbaalenii* PYR-1) and Gram-
17 35 negative (*Pseudomonas fluorescens*) bacteria exhibited distinct IR spectral alterations.
18 36 Multivariate analysis coupled with multivariate regression tree (MRT) indicates nutrient
19 37 depletion and exposure time as the primary factors in bacterial behaviour, followed by
20 38 exposure category and bacterial type. Nutrient depletion and starvation during long-term
21 39 exposure drives bacterial cells into a dormant state or to exhibit additional cellular
22 40 components (*e.g.*, fatty acids) in response to antimicrobials, consequently causing a broader
23 41 range of spectral alterations compared to short-term exposure. This work is the first report
24 42 highlighting the more important roles of exposure duration and nutrient depletion, instead of
25 43 treatment regimen of antimicrobial, on microbial responses to low-level and prolonged
26 44 environmental exposures.
27
28
29
30
31
32
33
34
35
36
37
38
39
40
41
42
43
44
45

1. Introduction

Environmental exposure to antimicrobials is a critical issue for both human and microbial communities. Antibiotics are currently ranked as the third most commonly prescribed drugs¹. In human and veterinary medicine there is abuse of antibiotics, especially for keeping animals healthy at a sub-therapeutic level²⁻⁹. The primary sink for such antibiotic usage is the environment, *e.g.*, waters and soils, *via* various pathways post-excretion^{2,3 4, 6}. Another group of frequently-used antimicrobial agents is silver-associated entities. Notably, unlike silver ion or salts whose antimicrobial effects are well-studied, the mechanisms of nanoparticulate silver (AgNP) activity remain unclear. However, AgNP is widely exploited for its antibacterial activity, in clothing, food containers, wound dressings, ointments, implant coatings, and ultrafiltration membranes for water purification¹⁰⁻¹⁴. Developing a reliable approach to interrogate microbial responses to antimicrobials is therefore a matter of urgency, contributing to better understanding of the mechanisms and impacts of antimicrobial agents on environmental microbes¹⁵.

A major issue is the translation from laboratory culture to the real-world scenario of bacteria living in their natural habitats. In contrast to most laboratory culture conditions, *e.g.*, nutrient rich broth, free-living bacteria commonly face nutrient depletion or even more prohibitive circumstances¹⁶. For instance, cells inhabiting biofilm may be exposed to different concentrations of nutrients, metabolites or environmental stimuli (*e.g.*, temperature, pH, oxygen, etc.)¹⁷⁻²¹ across the biofilm matrix and local microenvironment, leading to heterogeneous growth rates and behaviours amongst the cell populations^{22, 23}. Amongst these, a small proportion might differentiate into a highly protected phenotypic state and coexist with neighbouring populations that are antibiotic sensitive, resulting from inherent strain differences and adaptation to relatively low concentrations of exposure^{16, 22, 23}. Moreover, although regulatory agencies and pharmaceutical administration generally employs high doses of antimicrobials in *in-vivo* and *in-vitro* trials to ensure the safety of test chemicals, residual exposure is typically associated with extremely low-levels in the physical environment; this raises question as to whether high-concentrations of exposure represent the real-world outcomes²⁴⁻²⁹. Thus, research on prolonged low-level exposures of antimicrobials is required in order to shed deeper insights into microbial responses to antimicrobials in the real-world environment¹⁵.

1
2
3 77 Despite recently developed molecular techniques towards targeting microbial
4 78 phenotypes, such approaches to identify minor or pre-stage phenotypic alterations induced by
5 79 low-level exposure remain limited³⁰⁻³³. Meanwhile, other confounding factors (*e.g.*, microbial
6 79 species, growth phase, exposure time, etc.) may also influence test results^{16, 31, 34}. In 1991,
7 80
8 80 Fourier-transform infrared (FTIR) spectroscopy was innovatively introduced as a sensitive
9 81
10 81 and rapid screening tool for the characterization, classification and identification of
11 82
12 82 microorganisms¹⁶. Since then, the emerging application of spectrochemical techniques with
13 83
14 83 computational analysis as an inter-discipline approach shows promising feasibility in
15 84
16 84 microbiology and cytology³⁰⁻³⁶. In the last decade, FTIR spectroscopy plus chemometrics has
17 85
18 85 been exploited broadly for identifying microbial identities, physiologies, activities and related
19 86
20 86 functions^{16, 30, 31, 33, 34, 37, 38}. This technical combination provides a major advantage in terms
21 87
22 87 of being high-throughput, label-free and cost-effective in application³⁰, allowing one to
23 88
24 88 interrogate biological samples *via* a nondestructive and nonintrusive manner, which has great
25 89
26 89 potential in monitoring real-world scenarios^{30-32, 34}.

26 91 The current study applied attenuated total reflection FTIR (ATR-FTIR) microscopy
27 92 coupled with multivariate analysis to investigate bacterial responses to prolonged low-level
28 93 exposures of AgNP and tetracycline under nutrient depletion conditions. Compared to short-
29 94 term exposure, we found that length of exposure plays a more important role than treatment
30 95 with antimicrobial reagents or bacterial type, further uncovering key influential factors of
31 96 bacterial responses to antimicrobials during cell growth associated with nutrient depletion.

36 97 2. Methodology

38 98 2.1 Cell strains and sample preparation

39 99 The two bacterial strains used in this study were *Mycobacterium vanbaalenii* PYR-1 (Gram-
40 100 positive) and *Pseudomonas fluorescens* (Gram-negative). They were both grown in minimal
41 101 medium with 20 mM sodium succinate, undertaken in a dark rotary shaker at 150 rpm and the
42 102 culture temperature was 30±2°C. After centrifugation and washing with sterile water, cell
43 103 pellets were diluted in fresh minimal medium with 20 mM sodium succinate and cultivated
44 104 for about 2 h until they reached the early log-phase (CFU=1×10⁷ cells/mL). The four
45 105 treatments included non-exposure negative control (CK), 4 µg/L of AgNP, 1 µg/L of
46 106 tetracycline, and a mixture with 4 µg/L of AgNP and 1 µg/L of tetracycline (Binary). The
47 107 concentrations of AgNP and tetracycline were selected according to their previous reported
48 108 level in natural environment to mimic the low-level exposure in real-world scenario³⁸. They

1
2
3 109 are about 2-4 orders of magnitude lower than the minimum inhibitory concentration (MIC) of
4 110 AgNP (1 to 10 mg/L)^{39, 40} and tetracycline (1 to >30 mg/L)^{41, 42}, and therefore do not inhibit
5 111 bacterial growth. The samples of short-term exposure were taken after 2 h (late log-phase, T₀)
6 112 and 48 h (T₁), respectively. To create a nutrient-depletion condition for long-term exposure,
7 113 the cells were cultivated in 10-times diluted minimal medium and the culture medium was
8 114 refreshed every 72 h. The samples were collected at 3 (T₂), 6 (T₃), 9 (T₄) and 12 (T₅) days.
9 115 The collected cells were then harvested by centrifugation at 4000 rcf for 5 min, washed three
10 116 times with sterile deionized water, and finally fixed with 70% ethanol to prevent further
11 117 exposure.

18 118 2.2 Spectrochemical analysis

19
20 119 The prepared samples (minimal amount > 5 µL) were then applied onto Low-E slides and
21 120 dried for analysis by ATR-FTIR spectroscopy. A Bruker TENSOR 27 FTIR spectrometer
22 121 (Bruker Optics Ltd., UK) with a Helios ATR attachment containing a diamond internal
23 122 reflection element (IRE) was applied to acquire IR spectra. The data were attained at a
24 123 resolution of 3.84 cm⁻¹, 2.2 kHz mirror velocity and 32 co-additions. The instrument
25 124 parameters were set at 32 scans and 16 cm⁻¹ resolution. To collect the data, a total of 30
26 125 individual spectral measurements were taken randomly from each sample using the aid of the
27 126 ATR magnification-limited viewfinder camera. Prior to analysing each new specimen, the
28 127 crystal was cleaned using deionized water and a background reading was taken.

35 128 2.3 Multivariate analysis and statistics

36
37 129 All the initial data generated from ATR-FTIR spectroscopy were analysed using MATLAB
38 130 R2011a (*TheMathsWorks, Natick, MA, USA*) coupled with the IRootLab toolbox
39 131 (<http://irootlab.googlecode.com>)⁴³. The acquired IR spectra were merged and cut to the
40 132 biochemical-cell fingerprint region (1800-900 cm⁻¹). Then a rubber-band baseline correction
41 133 was applied to remove any slopes in this area. The data were then normalized to Amide I
42 134 (1650 cm⁻¹) and the means were centered allowing alignment of the different spectra for
43 135 comparison.

44
45 136 Principal component analysis-linear discriminant analysis (PCA-LDA) was applied
46 137 after data pre-processing to reduce the number of spectra to 10 uncorrelated principal
47 138 components (PCs), which account for >99% of the total variance. LDA is a supervised
48 139 technique coupled with PCA in order to maximize interclass and minimize intraclass
49 140 variance^{30, 31, 44}. Cross-calculation was subsequently performed to mitigate risks resulting from

1
2
3 141 LDA overfitting⁴⁵. The PCA-LDA loadings using ($n-1$) samples (n = number of samples in
4 142 dataset) was trained *via* leave-one-out cross-validation and then calculated the scores of the
5
6 143 rest sample. This process was performed for all scores within the test.

7
8 144 PCA-LDA cluster vectors are pseudo-spectra highlighting the key biochemical
9 145 alterations of each group in the dataset³⁵, which allows one to simplify the identification of
10 146 discriminating differences amongst groups. The centre of the control cluster itself is moved to
11 147 the origin of the PCA-LDA factor space. The extent of peak deviation away from the origin
12 148 of the factor space then occurs according to the centre of each corresponding agent-induced
13 149 cluster, proportional to the discriminating extent of biochemical differences^{31, 45}. Cluster
14 150 vectors plots were also applied to indicate the most prominent six significant peaks.

15
16 151 Multivariate regression trees (MRT) were used to analyse the influence of bacterial
17 152 type, exposure time and exposure category on biospectral alterations using the R package
18 153 “mvpart”. Herein, Gram-positive (*M. vanbaalenii*) and Gram-negative (*P. fluorescens*) strains
19 154 were assigned as 1 and 0. The exposure of AgNP, tetracycline and their mixtures were
20 155 assigned as 1, 2 and 3, respectively. The samples collected at different time points (T_0 , T_1 , T_2 ,
21 156 T_3 , T_4 and T_5) were assigned to 1, 2, 3, 4, 5 and 6, respectively.

22
23 157 One-way analysis of variance (ANOVA) with Tukey’s post-hoc test/or *t*-test was
24 158 employed to test the differences between treatments. All statistical analyses were carried out
25 159 in GraphPad Prism 6.

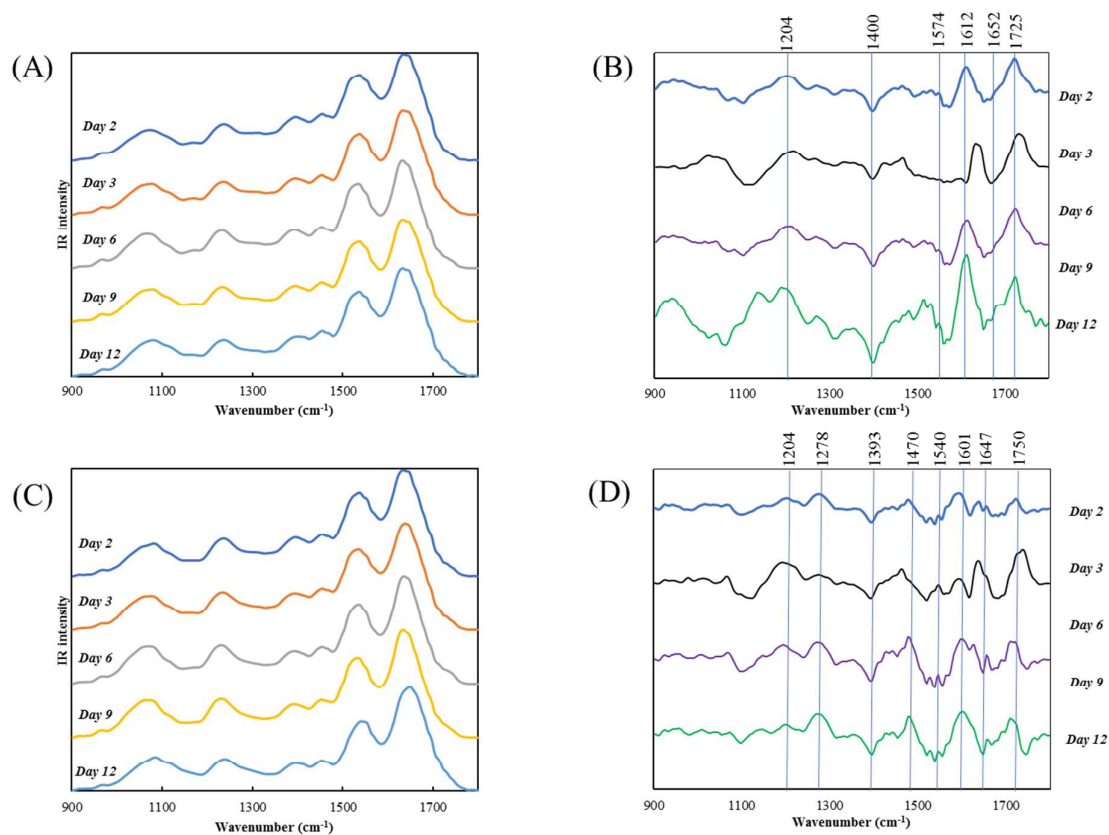
26 160 3. Results and discussion

27 161 3.1 Growth-dependent spectrochemical alterations

28 162 Throughout the study, a spectral class mean for the bacterial control group has been derived,
29 163 which generates an average spectrum based on all raw data from the same group. However,
30 164 minor variability is visualised from the class mean data directly between groups at different
31 165 time points (Figure 1A and 1B). Although previous studies suggest that bacteria with limited
32 166 nutrients are more likely to enter a dormant state waiting suitable growth conditions^{46, 47}, the
33 167 spectral alterations induced by nutrient depletion are limited. Therefore, a further cluster
34 168 vectors analysis is applied to highlight the minor alterations derived from nutrient depletion
35 169 (Figure 1C and 1D). The identical spectral biomarkers in both Gram-positive (*M. Vanbaalenii*)
36 170 and Gram-negative (*P. fluorescens*) bacteria are associated with Amide I, Amide III (~1204
37 171 cm^{-1} , ~1647 cm^{-1})^{30, 33} (Table 1). The main changes appearing in *M. Vanbaalenii* are Amide

1
2
3 172 III, ($\sim 1204\text{ cm}^{-1}$, $\sim 1400\text{ cm}^{-1}$), C=N adenine ($\sim 1574\text{ cm}^{-1}$), Amide I ($\sim 1652\text{ cm}^{-1}$), and C=O
4 173 band ($\sim 1725\text{ cm}^{-1}$)^{33, 48}. Of these, the amino acid-associated alterations possibly contributing
5
6 174 to nucleotide metabolism, which is important for cellular catabolism are significant. Along
7
8 175 with long-term starvation and oxygen depletion, decreasing amounts of nucleotides are
9
10 176 associated with reduced cell activities and replication compared to log-phase. Furthermore,
11
12 177 alterations in other cellular components (*e.g.*, proteins) might be mainly responsible for cell
13
14 178 wall maintenance, based on previous study⁴⁹.

15 179 The specific spectrochemical alterations of *P. fluorescens* include Amide III (~ 1278
16
17 180 cm^{-1}), CH₂ bending of the methylene chains in lipids ($\sim 1470\text{ cm}^{-1}$), protein Amide II
18
19 181 absorption ($\sim 1540\text{ cm}^{-1}$), C=N cytosine ($\sim 1601\text{ cm}^{-1}$), $\nu(\text{C}=\text{C})$ lipids, and fatty acids (~ 1750
20
21 182 cm^{-1})^{34, 48}. Accordingly, more lipid alterations under nutrient depletion conditions are found
22
23 183 in Gram-negative *P. fluorescens* versus Gram-positive *M. vanbaalenii* owing to their
24
25 184 differing cell wall structures. There is only a thin peptidoglycan layer ($\sim 2\text{-}3\text{ nm}$) between the
26
27 185 cytoplasmic and outer membrane in Gram-negative bacteria, whereas the outer membrane in
28
29 186 Gram-positive bacteria is a thick peptidoglycan layer of 30 nm with no other additional
30
31 187 structure⁵⁰. The attributes of membrane structure may explain the distinct spectrochemical
32
33 188 alterations between *P. fluorescens* and *M. vanbaalenii* under nutrient depletion, which might
34
35 189 lead to different responses towards long-term exposure of antimicrobials.
36
37
38
39
40
41
42
43
44
45
46
47
48
49
50
51
52
53
54
55
56
57
58
59
60



190

191 **Figure 1.** Spectrochemical alterations with length of culture. Infrared spectra of *M.*
 192 *vanbaalenii* (A) and *P. fluorescens* (C) from control group. Cluster vectors plots of *M.*
 193 *vanbaalenii* (B) and *P. fluorescens* (D) from control group, indicating significant
 194 wavenumbers contributing to segregating spectral alterations that develop with increasing
 195 culture time.

Table 1. Spectrochemical profile regarding the significant spectral biomarkers peaks derived from cluster vectors of *M. vanbaalenii* (Gram-positive) and *P. fluorescens* (Gram-negative) post-exposure to AgNP, tetracycline and their mixtures. Red dots represent identical biomarkers for both Gram-positive and Gram-negative bacteria, and green and blue dots indicate biomarkers appear only in Gram-positive or Gram-negative bacteria, respectively.

Wavenumber (cm ⁻¹)	Annotation	Gram-positive				Gram-negative			
		Growth	AgNP	Tetracycline	Binary	Growth	AgNP	Tetracycline	Binary
~ 964	C-C, C-O deoxyribose	-	●	-	-	-	-	-	-
~ 1084	DNA	-	-	●	●	-	-	-	-
~ 1204	Amide III	●	-	-	-	●	-	-	-
~ 1212	Phosphate	-	●	-	-	-	-	-	-
~ 1220	PO ₂ ⁻ stretching in RNA and DNA	-	-	●	●	-	-	●	-
~ 1278	Amide III	-	-	-	-	●	-	-	-
~ 1307	Amide III	-	●	-	●	-	-	-	-
~ 1327	Stretching C-N thymine, adenine	-	-	-	-	-	●	-	●
~ 1393		-	-	-	-	●	-	-	-
~ 1400		●	-	-	-	-	-	-	-
~ 1404	CH ₃ asymmetric deformation	-	-	-	●	-	-	-	-
~ 1423		-	-	-	-	-	●	●	●
~ 1458	Lipids and proteins	-	-	-	-	-	-	●	-
~ 1462		-	-	-	●	-	-	-	●
~ 1468		-	-	-	-	-	●	-	-
~ 1470	CH ₂ bending of the methylene chains in lipids	-	-	-	-	●	-	-	-
~ 1477		-	-	●	-	-	-	-	-
~ 1520	Amide II	-	-	-	-	-	-	-	●
~ 1540	Protein amide II absorption	-	-	-	-	●	-	-	-
~ 1555	Ring base	-	●	●	●	-	-	-	-
~ 1574	C=N adenine	●	-	-	-	-	-	-	-
~ 1577	C-C stretch	-	-	-	-	-	●	-	-

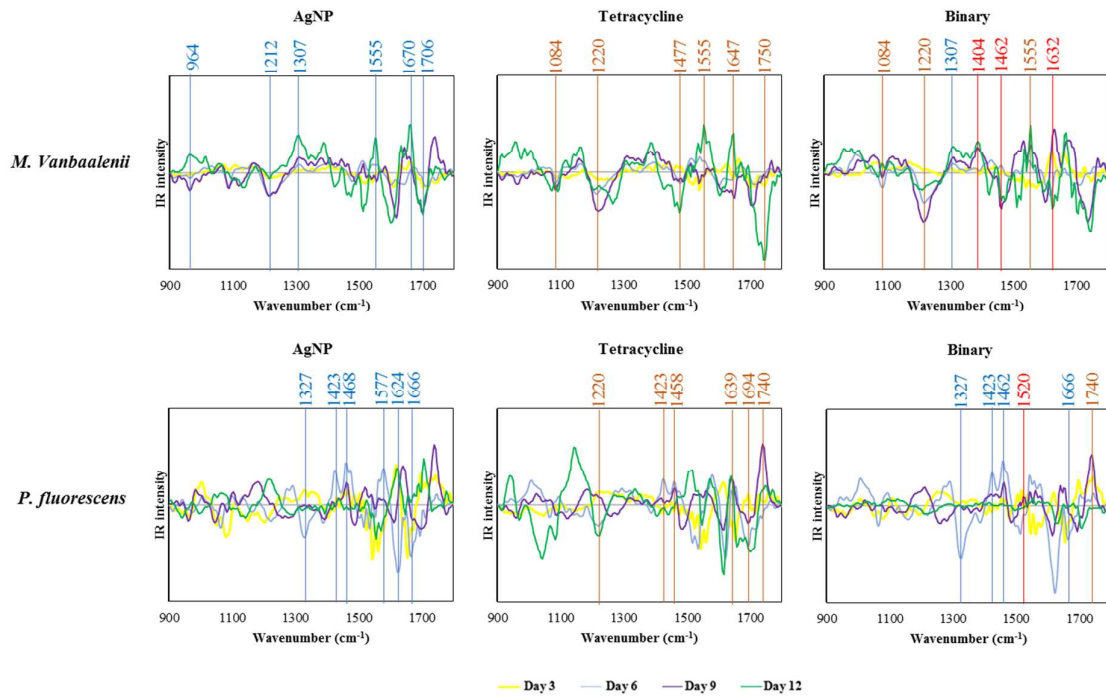
1
2
3
4
5
6
7
8
9
10
11
12
13
14
15
16
17
18
19
20
21
22
23
24
25
26
27
28
29
30
31
32
33
34
35
36
37
38
39
40
41
42
43
44
45
46
47

~ 1601	C=N cytosine	-	-	-	-	●	-	-	-
~ 1612		●	-	-	-	-	-	-	-
~ 1624		-	-	-	-	-	●	-	-
~ 1632	C-C stretch	-	-	-	●	-	-	-	-
~ 1639	Amide	-	-	-	-	-	-	●	-
~ 1647	Amide I	-	-	●	-	●	-	-	-
~ 1652	Amide I	●	-	-	-	-	-	-	-
~ 1666	C=O stretching vibration of pyrimidine base	-	-	-	-	-	●	-	●
~ 1670	Amide I	-	●	-	-	-	-	-	-
~ 1694	Proteins	-	-	-	-	-	-	●	-
~ 1706	C=O thymine	-	●	-	-	-	-	-	-
~ 1725	C=O band	●	-	-	-	-	-	-	-
~ 1740	C=O, lipids	-	-	-	-	-	-	●	●
~ 1750	v(C=C) lipids, fatty acids	-	-	●	-	●	-	-	-

200

201 3.2 Spectrochemical alterations with long-term AgNP/tetracycline exposure

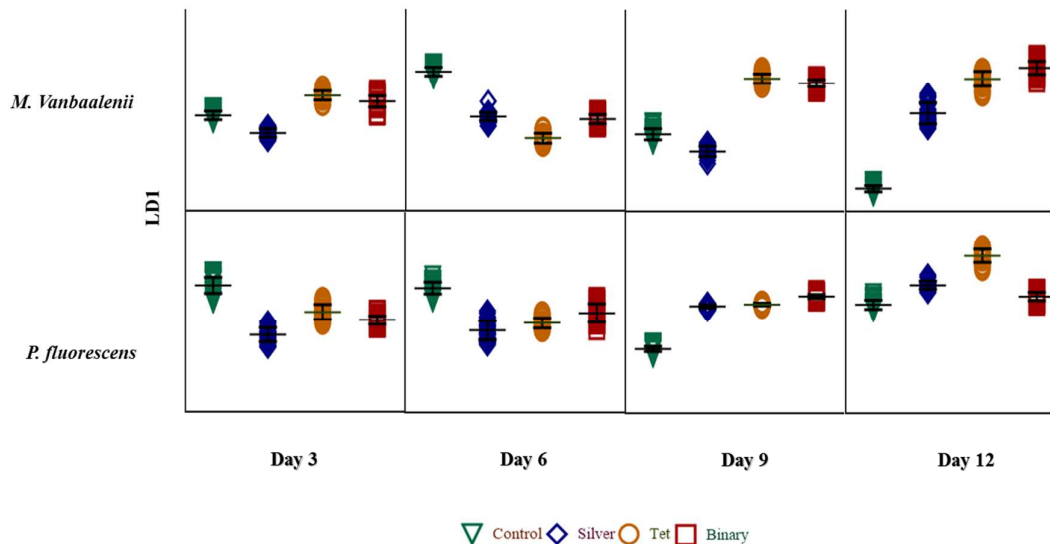
202 To identify exposure-induced alterations, the spectral data of each treatment group are
203 compared with the control group at the same time point, eliminating the impacts of cell
204 growth and nutrient depletion (Figure 2). In Gram-positive *M. Vanbaalenii*, the AgNP-
205 induced alterations are C-C, C-O deoxyribose ($\sim 964\text{ cm}^{-1}$), phosphate ($\sim 1212\text{ cm}^{-1}$), Amide
206 III ($\sim 1307\text{ cm}^{-1}$), ring base ($\sim 1555\text{ cm}^{-1}$), Amide I ($\sim 1670\text{ cm}^{-1}$), and C=O thymine (~ 1706
207 cm^{-1})^{30, 33, 38}. Post-exposure to tetracycline, the representative peaks are DNA ($\sim 1084\text{ cm}^{-1}$),
208 PO_2^- stretching in RNA and DNA ($\sim 1220\text{ cm}^{-1}$), ring base ($\sim 1555\text{ cm}^{-1}$), Amide I (~ 1647
209 cm^{-1}), lipids, and fatty acids ($\sim 1750\text{ cm}^{-1}$)^{33, 38, 48}. With the binary exposure, the alterations
210 are different from individual exposures, and the specific spectral biomarkers are DNA (~ 1084
211 cm^{-1}), PO_2^- stretching in RNA and DNA ($\sim 1220\text{ cm}^{-1}$), Amide III ($\sim 1307\text{ cm}^{-1}$), CH_3
212 asymmetric deformation ($\sim 1404\text{ cm}^{-1}$, $\sim 1462\text{ cm}^{-1}$), ring base ($\sim 1555\text{ cm}^{-1}$), and C-C stretch
213 ($\sim 1632\text{ cm}^{-1}$)^{38, 48}. It is worth mentioning that the binary effects of AgNP and tetracycline on
214 *M. vanbaalenii* spectra are mainly driven by tetracycline as more identical discriminating
215 peaks are observed between these two groups (Table 1). To evaluate the impacts of each
216 exposure, PCA-LDA score plots were generated and illustrate the increasing segregation
217 between groups with increasing exposure time (from day 3 to day 12, Figure 3). Particularly,
218 the biochemical distances of tetracycline and binary groups are co-located, apparently
219 separated from the control group and markedly on day 12. However, the AgNP-treated
220 groups only show slight shifting of biochemical differences compared to the control group.
221 This result is consistent with cluster vectors analysis that the binary-exposure effects in *M.*
222 *vanbaalenii* are closer to tetracycline alone than AgNP.



223

224 **Figure 2.** Cluster vectors plots after PCA-LDA, indicating significant wavenumbers for the
 225 segregation of *M. vanbaalenii* and *P. fluorescens* following long-term exposure (day 3 to day
 226 12) to AgNP, tetracycline or their mixtures.

227



228

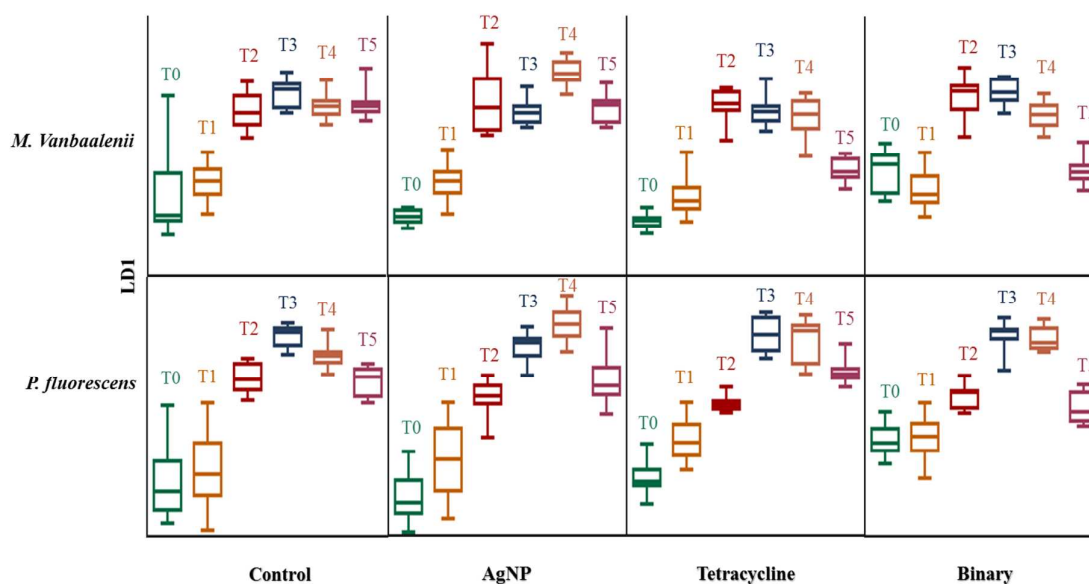
229 **Figure 3.** PCA-LDA score plots for the biospectral alteration of *M. vanbaalenii* and *P.*
 230 *fluorescens* following long-term exposure (day 3 to day 12) to AgNP, tetracycline or their
 231 mixtures.

232 In Gram-negative *P. fluorescens*, all the exposure groups are clearly separated from the
233 control group in the PCA-LDA score plots (Figure 3), and there is no significant difference
234 between each treatment. The AgNP-induced alterations include stretching C-N thymine,
235 adenine ($\sim 1327\text{ cm}^{-1}$), lipids and proteins ($\sim 1458\text{ cm}^{-1}$), C-C stretch ($\sim 1577\text{ cm}^{-1}$), (~ 1624
236 cm^{-1}), and C=O stretching vibration of pyrimidine base ($\sim 1666\text{ cm}^{-1}$)⁴⁸. The tetracycline-
237 induced peaks are DNA ($\sim 1220\text{ cm}^{-1}$); ($\sim 1423\text{ cm}^{-1}$), collagen ($\sim 1458\text{ cm}^{-1}$), Amide I (~ 1639
238 cm^{-1} , $\sim 1694\text{ cm}^{-1}$), and C=O lipids ($\sim 1740\text{ cm}^{-1}$)^{38, 48}. Generally, outer cellular components
239 are widely affected by both AgNP and tetracycline, including Amides I/II and proteins
240 ($\sim 1307\text{ cm}^{-1}$, $\sim 1647\text{ cm}^{-1}$, $1639-1694\text{ cm}^{-1}$), and lipids and/or fatty acids (1750 cm^{-1} , 1458
241 cm^{-1} , 1740 cm^{-1})^{30, 33, 38, 48}, indicating that the cell membrane is the primary reactive target
242 associated with both antimicrobials which penetrate bacterial cells *via* passive diffusion and
243 inhibit bacterial growth by perturbing protein synthesis or altering membrane structure⁵¹.
244 Additionally, more inner cellular components are identified to be associated with tetracycline
245 exposure than AgNP, *e.g.*, inherent DNA and RNA, possibly due to the antibiotic mechanism
246 of tetracycline which blocks the elongation cycle by preventing incoming aminoacyl-tRNA
247 (aa-tRNA) from binding to the ribosomal A-site and inhibiting protein synthesis⁵². Different
248 from Gram-positive strains, AgNP-induced alterations contribute predominantly to the binary
249 effects in *P. fluorescens*, *i.e.*, stretching C-N thymine, adenine ($\sim 1327\text{ cm}^{-1}$, $\sim 1423\text{ cm}^{-1}$,
250 $\sim 1462\text{ cm}^{-1}$), Amide II ($\sim 1520\text{ cm}^{-1}$), C=O stretching vibration of pyrimidine base (~ 1666
251 cm^{-1}), and C=O lipids ($\sim 1740\text{ cm}^{-1}$)^{31, 34}. These findings imply the antimicrobial synergism
252 of AgNP and tetracycline. A previous study suggests that antibiotics' efficacy against
253 microbes may increase in the presence of AgNP because of the bonding reaction between
254 antibiotics and nanofillers, owing to the chelating reaction of hydroxyl and amide groups in
255 antibiotic molecules with AgNP⁵³.

256 3.3 Impacts of exposure time on spectrochemical alterations

257 Although short-term impacts by antimicrobials on bacteria is obvious and well-studied, their
258 consequences may last for extended periods and remain unknown⁵⁴. To unravel such long-
259 term exposure effects, we measured the biospectral alterations at different time points, and
260 found distinguishing biomarkers post-exposure to antimicrobials between short-term *versus*
261 long-term treatments (Figure 4). Generally, in short-term exposure (≤ 3 days), spectral
262 changes are associated with components from cell membranes wherein most antimicrobial-
263 induced alterations occur in both strains, including glycogen ($\sim 1022\text{ cm}^{-1}$), symmetric
264 phosphate stretching vibrations ($\nu_s\text{PO}_2^-$; $\sim 1088\text{ cm}^{-1}$, 1092 cm^{-1}), carbohydrates (~ 1165

265 cm^{-1}), protein phosphorylation ($\sim 964 \text{ cm}^{-1}$), Amide I ($\sim 1609 \text{ cm}^{-1}$, 1612 cm^{-1} , 1659 cm^{-1} ,
 266 $\sim 1670 \text{ cm}^{-1}$), Amide III ($\sim 1269 \text{ cm}^{-1}$), COO- symmetric stretching vibrations of fatty acids
 267 and amino acid ($\sim 1408 \text{ cm}^{-1}$), proteins ($\sim 1485 \text{ cm}^{-1}$, $\sim 1550 \text{ cm}^{-1}$, $\sim 1650 \text{ cm}^{-1}$), and lipids
 268 ($\sim 1701 \text{ cm}^{-1}$, $1705\text{-}1750 \text{ cm}^{-1}$)^{30, 32, 38, 48}. Besides external cellular components, some
 269 inherent elements are significantly influenced in long-term exposure (>3 days). For instance,
 270 long-term tetracycline-induced alterations in *P. fluorescens* include RNA and DNA (e.g.,
 271 $\sim 1220 \text{ cm}^{-1}$, $\sim 1423 \text{ cm}^{-1}$). Compared to prolonged exposure, short exposure induces minimal
 272 alterations, possibly owing to bacteria undergoing pre-stage reactions against antimicrobials.
 273 During extended exposure periods, the more obvious biospectral alterations might be
 274 explained by increasing tetracycline accumulation *via* penetration and stronger antibiotic
 275 effects, which prevent RNA binding to the ribosomal A-site and protein synthesis⁵², and
 276 further inhibit RNA/DNA synthesis and duplication⁵⁵. Another explanation is the post-
 277 antibiotic effect (PAE) or lag of bacterial regrowth induced by long-term antimicrobial
 278 exposure, driving bacterial entry into a growth suppression state^{56, 57}.



279

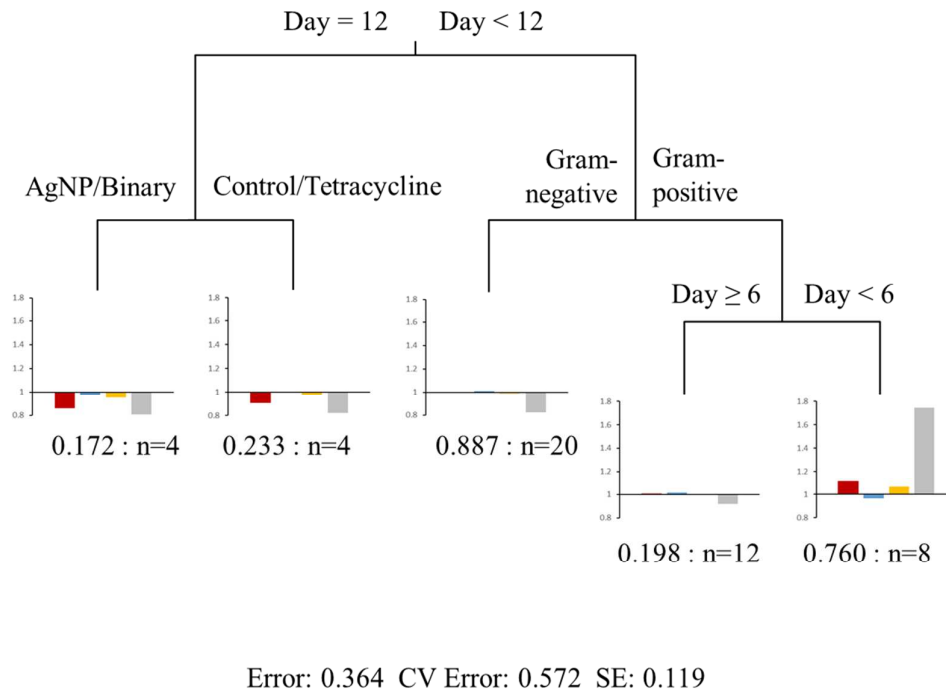
280 **Figure 4.** PCA-LDA score plots of the biospectral alteration of *M. vanbaalenii* and *P.*
 281 *fluorescens* in both short-term and long-term exposure to AgNP, tetracycline and their
 282 mixtures. T₀, T₁, T₂, T₃, T₄ and T₅ represent exposure time of 2 h, 2 days, 3 days, 6 days, 9
 283 days and 12 days, respectively.

284

285 3.4 Influential factors determining bacterial long-term responses to antimicrobials

286 Although distinct impacts of different antimicrobials on bacteria have been well-documented,
287 many variables including intrinsic and external factors may alter such influences in real-
288 world scenarios. In the present study, we evaluated bacterial type, exposure category,
289 exposure time and nutrient depletion, but which factor is the most dominating remains
290 unclear. To answer this question, a multivariate regression trees (MRT) analysis based on
291 isolated discriminating biomarkers is conducted to quantify the impacts of these four factors
292 on spectral alterations. MRT visualizes these influencing factors on spectral variations in a
293 tree with four splits based on exposure time, exposure category, bacterial type and nutrient
294 depletion, explaining 63.7% of the total spectral variance (Figure 5). Level of influence is
295 ranked as exposure time > exposure type > bacterial type = nutrient depletion. Exposure time
296 accounts for 17.8% of the total variance, with the first split separating the group of 12-day
297 exposure owing to the relatively lower intensities of DNA. In the 12-day exposure group,
298 exposure category explains 16.1% of the variance and splits spectra into two groups of
299 control/tetracycline and AgNP/binary, mainly based on DNA spectral biomarkers. The group
300 of exposure <12 days is further split by bacterial type, accounting for 14.9% of the total
301 variance and attributed to differences in DNA, phospholipid-derived fatty acids and proteins.
302 The final split representing nutrient depletion separates the groups of 6-9 day and 0-3 day for
303 Gram-positive bacteria (*M. vanbaalenii*, 14.9%), owing to higher cellular activities reflected
304 by significant variations in DNA, phospholipid-derived fatty acids and proteins.

305 The MRT results are consistent with PCA-LDA score plots (Figure 4). The spectral
306 distances of *P. fluorescens*, for instance, are similar regardless of exposure categories from
307 day 9 due to cell regeneration against the exposure and exhibiting resistance to
308 antimicrobials⁴⁶. A prior study reported that long-term exposure (5 days) to 1 µg/L of
309 tetracycline shows no apparent effect on cyanobacterial cells due to their natural variability in
310 tetracycline resistance⁵⁸. It might explain the closer distance between groups of control and
311 tetracycline. Moreover, the distinct behaviours of *M. vanbaalenii* and *P. fluorescens* upon
312 starvation can explain the fourth split in MRT, *i.e.*, *M. vanbaalenii* enters a replicative state
313 after 6-day exposure to adapt to conditions of insufficient nutrients, whereas *P. fluorescens*
314 appears more susceptible to nutrient depletion and starts regrowth. Evidence can be found
315 from the additional cellular components produced in Gram-negative *P. fluorescens*, *e.g.*, fatty
316 acids (~1750 cm⁻¹), as their predominant energy to survive⁴⁶.



317

318 **Figure 5.** Multivariate regression tree (MRT) analysis of environmental variables explaining
 319 discriminating biomarkers. The scale of the sub-figures reflects the alteration degree (number
 320 one represents the average level). Red bars represent biomarkers assigned to DNA; blue bars
 321 represent biomarkers associated with proteins; yellow bars represent biomarkers assigned to
 322 phospholipid-derived fatty acids; and, grey bars represent other cellular components.

323

324 Moreover, bacterial type may also have impacts on the consequences posed by antimicrobials
 325 since bacteria differ in their cellular structures. Antimicrobials acting as both efficient
 326 eliminators to microbes and selective agents help to propagate organisms with resistance
 327 ability⁵⁹. Herein, we found discriminating alterations between Gram-positive and Gram-
 328 negative strains within the same exposure treatment. All the treatments exhibit distinct
 329 alterations in Gram-positive *M. vanbaalenii* under nutrient depletion conditions (Day 3 to
 330 Day 12), although AgNP generates very limited impact as compared to tetracycline or binary
 331 exposure groups; these are not observed in *P. fluorescens*. The results from PCA-LDA scores
 332 plots (Figure 3) and MRT (Figure 5) also show induced alterations in *M. vanbaalenii* are
 333 significant compared to *P. fluorescens*. Furthermore, after long-term exposure (12 days),

1
2
3 334 Gram-negative *P. fluorescens* exhibit a broad range of spectral alterations assigned to lipids
4 335 and/or fatty acid (e.g., 1458 cm⁻¹, 1740 cm⁻¹), which are absent in Gram-positive *M.*
5 336 *vanbaalenii*, mainly attributed to their different cell wall structures. The rigidity and extended
6 337 cross-linking may reduce the target sites in cell membranes for environmental exposures and
7 338 afford further protection to cells from antimicrobial penetration^{12, 53}. It implies that cell
8 339 membranes of Gram-negative bacteria are more likely to be influenced compared to Gram-
9 340 positive bacteria under certain antibacterial treatments (e.g., AgNP)^{12, 50, 60}. Past studies report
10 341 the oxidation of smaller AgNPs (1-10 nm) by intercellular reactive oxygen species (ROS) in
11 342 Gram-negative bacteria, resulting in the release of silver ions during AgNP penetration
12 343 through the cell membrane and entrance into the cytoplasm⁶⁰. These silver ions could be
13 344 further transferred to other Gram-negative bacterial cells, the membrane and cytoplasm which
14 345 contain many sulfur-containing proteins for the released Ag⁺ to bind to and inactivate^{50, 60}.
15 346 Furthermore, it has been recognised that heavy metal treatment can induce global
16 347 biomolecular changes in lipids and proteins, implying exotic exposure may lead to the
17 348 development of relevant metabolic changes in cellular components, particularly the
18 349 membrane⁶¹⁻⁶³. A recent study, for instance, reported that Ag exposure could increase cellular
19 350 lipid contents while decrease membrane fluidity⁶¹, and the possible mechanism is upregulated
20 351 lipid biosynthesis, which is known to be associated with the reduced membrane permeability.

21
22
23
24
25
26
27
28
29
30
31
32
33 352 Besides bacterial type, exposure time and exposure category, nutrient depletion is also
34 353 found to be an influential factor in the bacterial antimicrobial response. Here, bacterial cells
35 354 tend to adapt to new environmental stimuli after entering into a long-term nutrient-deprived
36 355 situation. From the cluster vectors analysis (Figure 1), spectral alterations in both strains from
37 356 Day 6 show slight peak shifts, which can be regarded as a potential signal showing that
38 357 bacterial cells are undergoing adaption. Additionally, *M. vanbaalenii* becomes a persistent
39 358 suspension in the media on entering a dormant state from Day 6. This is because bacteria in a
40 359 non-growing state can survive for much longer time under conditions of reduced oxygen or
41 360 nutrient deprivation^{46, 47}. Upon starvation, bacterial cells fragment into small spheroids
42 361 exhibiting rapid and drastic decreases in endogenous metabolism. This reorganization gives
43 362 bacteria maximum survival during long-term starvation. Specifically, bacteria on starvation
44 363 initially induce dwarfing generating cell number increases *via* fragmentation over the first 1
45 364 to 2 h and continuous size reductions in the fragmented cells, but no further increase in
46 365 numbers. After dwarfing phases, cell size continues to get smaller, with little or no metabolic
47 366 activity, and slow loss of viability⁶⁴. It has been reported that non-growing phase bacteria

1
2
3 367 adapt to and increase their tolerance to environmental stresses and such developed persistent
4 368 bacilli are capable of surviving several months of combinatorial antibiotic treatment⁴⁷, which
5 369 implies that stressed living conditions, to some extent and paradoxically, could help microbial
6 370 resistance to antimicrobial effects.

371 **4. Conclusions**

372 In the present study, we employed spectrochemical analysis coupled with multivariate
373 analysis as a robust tool towards investigating bacterial responses to long-term and low-level
374 exposure of antimicrobials under nutrient depletion conditions. ATR-FTIR spectroscopy
375 shows feasibility in revealing sufficient biochemical information continuously even at
376 extremely low-level exposures in a starvation situation, which fits better with real-world
377 circumstances and the natural state of microcosms. From the multivariate analysis of spectra
378 coupled with MRT, we evaluate the significance of different factors on long-term bacterial
379 responses to antimicrobials and find pivotal roles for exposure time and nutrient depletion.
380 Nutrient depletion can drive bacterial cells to either enter into a dormant state or exhibit
381 extra-cellular components against environmental antimicrobials, consequently causing a
382 broader range of spectral alteration compared to short-term exposures. Differences in
383 bacterial behaviours towards antimicrobials are also found between bacterial types (Gram-
384 positive *versus* Gram-negative) attributed to variations in cell wall structure. Our work is the
385 first revealing of the more important roles of exposure duration and nutrient depletion, rather
386 than of antimicrobial reagents, on microbial responses to low-level and prolonged
387 environmental exposures. We believe this approach has an important future with potential
388 feasibility in *in situ* screening of environmental exposures in real-time.

389 **Conflicts of interest**

390 There are no conflicts of interest to declare.

391 **Acknowledgement**

392 N.J. was funded by Chinese Academy of Sciences and China Scholarship Council.

393

394

395

396 **References**

- 397 1. J. Conly, *Can. Med. Assoc. J.*, 2002, **167**, 885-891.
- 398 2. J. W. Harrison and T. A. Svec, *Quintessence Int.*, 1998, **29**, 223-229.
- 399 3. J. C. Chee-Sanford, R. I. Aminov, I. J. Krapac, N. Garrigues-Jeanjean and R. I.
400 Mackie, *Appl. Environ. Microbiol.*, 2001, **67**, 1494-1502.
- 401 4. G. Hamscher, S. Sczesny, H. Hoper and H. Nau, *Anal Chem*, 2002, **74**, 1509-1518.
- 402 5. X. L. Ji, Q. H. Shen, F. Liu, J. Ma, G. Xu, Y. L. Wang and M. H. Wu, *J. Hazard*
403 *Mater.*, 2012, **235**, 178-185.
- 404 6. L. Cantas, S. Q. A. Shah, L. M. Cavaco, C. M. Manaia, F. Walsh, M. Popowska, H.
405 Garelick, H. Burgmann and H. Sorum, *Front. Microbiol.*, 2013, **4**, 14.
- 406 7. A. Koluman and A. Dikici, *Crit. Rev. Microbiol.*, 2013, **39**, 57-69.
- 407 8. M. Tandukar, S. Oh, U. Tezel, K. T. Konstantinidis and S. G. Pavlostathis, *Environ.*
408 *Sci. Technol.*, 2013, **47**, 9730-9738.
- 409 9. J. L. Martinez and F. Baquero, *Ups. J. Med. Sci.*, 2014, **119**, 68-77.
- 410 10. J. S. Kim, E. Kuk, K. N. Yu, J. H. Kim, S. J. Park, H. J. Lee, S. H. Kim, Y. K. Park, Y.
411 H. Park, C. Y. Hwang, Y. K. Kim, Y. S. Lee, D. H. Jeong and M. H. Cho, *Nanomed.-*
412 *Nanotechnol. Biol. Med.*, 2014, **10**, 1119-1119.
- 413 11. C. N. Lok, C. M. Ho, R. Chen, Q. Y. He, W. Y. Yu, H. Sun, P. K. H. Tam, J. F. Chiu
414 and C. M. Che, *J. Biol. Inorg. Chem.*, 2007, **12**, 527-534.
- 415 12. H. H. Lara, N. V. Ayala-Nunez, L. D. I. Turrent and C. R. Padilla, *World J. Microbiol.*
416 *Biotechnol.*, 2010, **26**, 615-621.
- 417 13. C. Marambio-Jones and E. M. V. Hoek, *J. Nanopart. Res*, 2010, **12**, 1531-1551.
- 418 14. R. J. Griffitt, N. J. Brown-Peterson, D. A. Savin, C. S. Manning, I. Boube, R. A. Ryan
419 and M. Brouwer, *Environ. Toxicol. Chem.*, 2012, **31**, 160-167.
- 420 15. A. Gupta and S. Silver, *Nat. Biotechnol.*, 1998, **16**, 888-888.
- 421 16. N. F. Jin, D. Y. Zhang and F. L. Martin, *Integr. Biol.*, 2017, **9**, 406-417.
- 422 17. P. Marschner, C. H. Yang, R. Lieberei and D. E. Crowley, *Soil Biol Biochem*, 2001,
423 **33**, 1437-1445.
- 424 18. E. K. Costello, C. L. Lauber, M. Hamady, N. Fierer, J. I. Gordon and R. Knight,
425 *Science*, 2009, **326**, 1694-1697.
- 426 19. C. L. Lauber, M. Hamady, R. Knight and N. Fierer, *Appl. Environ. Microbiol.*, 2009,
427 **75**, 5111-5120.
- 428 20. M. Wietz, B. Wemheuer, H. Simon, H. A. Giebel, M. A. Seibt, R. Daniel, T.
429 Brinkhoff and M. Simon, *Environ. Microbiol.*, 2015, **17**, 3822-3831.
- 430 21. H. Li, F. L. Martin and D. Y. Zhang, *Anal. Chem.*, 2017, **89**, 3909-3918.
- 431 22. P. S. Stewart and J. W. Costerton, *Lancet*, 2001, **358**, 135-138.
- 432 23. N. Hoiby, T. Bjarnsholt, M. Givskov, S. Molin and O. Ciofu, *Int. J. Antimicrob.*
433 *Agents*, 2010, **35**, 322-332.
- 434 24. C. G. Mayhall and E. Apollo, *Antimicrob. Agents Chemother.*, 1980, **18**, 784-788.
- 435 25. M. R. W. Brown, D. G. Allison and P. Gilbert, *J. Antimicrob. Chemother.*, 1988, **22**,
436 777-780.
- 437 26. S. M. Ede, L. M. Hafner and P. M. Fredericks, *Appl. Spectrosc.*, 2004, **58**, 317-322.
- 438 27. O. I. Kalantzi, R. Hewitt, K. J. Ford, L. Cooper, R. E. Alcock, G. O. Thomas, J. A.
439 Morris, T. J. McMillan, K. C. Jones and F. L. Martin, *Carcinogenesis*, 2004, **25**, 613-
440 622.
- 441 28. J. L. Barber, M. J. Walsh, R. Hewitt, K. C. Jones and F. L. Martin, *Mutagenesis*, 2006,
442 **21**, 351-360.
- 443 29. O. Fridman, A. Goldberg, I. Ronin, N. Shores and N. Q. Balaban, *Nature*, 2014, **513**,
444 418-421.

- 1
2
3 445 30. F. L. Martin, J. G. Kelly, V. Llabjani, P. L. Martin-Hirsch, Patel, II, J. Trevisan, N. J.
4 446 Fullwood and M. J. Walsh, *Nat. Protoc.*, 2010, **5**, 1748-1760.
5 447 31. M. J. Riding, F. L. Martin, J. Trevisan, V. Llabjani, Patel, II, K. C. Jones and K. T.
6 448 Semple, *Environ. Pollut.*, 2012, **163**, 226-234.
7 449 32. J. Li, R. Strong, J. Trevisan, S. W. Fogarty, N. J. Fullwood, K. C. Jones and F. L.
8 450 Martin, *Environ. Sci. Technol.*, 2013, **47**, 10005-10011.
9 451 33. M. J. Baker, J. Trevisan, P. Bassan, R. Bhargava, H. J. Butler, K. M. Dorling, P. R.
10 452 Fielden, S. W. Fogarty, N. J. Fullwood, K. A. Heys, C. Hughes, P. Lasch, P. L.
11 453 Martin-Hirsch, B. Obinaju, G. D. Sockalingum, J. Sule-Suso, R. J. Strong, M. J.
12 454 Walsh, B. R. Wood, P. Gardner and F. L. Martin, *Nat. Protoc.*, 2014, **9**, 1771-1791.
13 455 34. K. A. Heys, M. J. Riding, R. J. Strong, R. F. Shore, M. G. Pereira, K. C. Jones, K. T.
14 456 Semple and F. L. Martin, *Analyst*, 2014, **139**, 896-905.
15 457 35. J. G. Kelly, J. Trevisan, A. D. Scott, P. L. Carmichael, H. M. Pollock, P. L. Martin-
16 458 Hirsch and F. L. Martin, *J. Proteome Res.*, 2011, **10**, 1437-1448.
17 459 36. J. Trevisan, P. P. Angelov, P. L. Carmichael, A. D. Scott and F. L. Martin, *Analyst*,
18 460 2012, **137**, 3202-3215.
19 461 37. N. Jin, M. Paraskevaidi, K. T. Semple, F. L. Martin and D. Y. Zhang, *Anal Chem*,
20 462 2017, **89**, 9814-9821.
21 463 38. N. Jin, K. T. Semple, L. Jiang, C. Luo, D. Zhang and F. L. Martin, *Analyst*, 2018, **143**,
22 464 768-776.
23 465 39. S. N. El Din, T. A. El-Tayeb, K. Abou-Aisha and M. El-Azizi, *Int. J. Nanomed.*, 2016,
24 466 **11**, 1749-1758.
25 467 40. A. J. Kora and J. Arunachalam, *World J. Microbiol. Biotechnol.*, 2011, **27**, 1209-1216.
26 468 41. J. T. H. Jo, F. S. L. Brinkman and R. E. W. Hancock, *Antimicrob. Agents Chemother.*,
27 469 2003, **47**, 1101-1111.
28 470 42. H. Wu, X. Shi, H. Wang and J. Liu, *J. Antimicrob. Chemother.*, 2000, **46**, 121-123.
29 471 43. J. Trevisan, P. P. Angelov, A. D. Scott, P. L. Carmichael and F. L. Martin,
30 472 *Bioinformatics*, 2013, **29**, 1095-1097.
31 473 44. F. L. Martin, M. J. German, E. Wit, T. Fearn, N. Ragavan and H. M. Pollock, *J.*
32 474 *Comput. Biol.*, 2007, **14**, 1176-1184.
33 475 45. J. Li, G. G. Ying, K. C. Jones and F. L. Martin, *Analyst*, 2015, **140**, 2687-2695.
34 476 46. J. C. Betts, P. T. Lukey, L. C. Robb, R. A. McAdam and K. Duncan, *Mol. Microbiol.*,
35 477 2002, **43**, 717-731.
36 478 47. T. Hampshire, S. Soneji, J. Bacon, B. W. James, J. Hinds, K. Laing, R. A. Stabler, P.
37 479 D. Marsh and P. D. Butcher, *Tuberculosis*, 2004, **84**, 228-238.
38 480 48. Z. Movasaghi, S. Rehman and I. U. Rehman, *Appl. Spectrosc. Rev.*, 2008, **43**, 134-
39 481 179.
40 482 49. M. Drapal, P. R. Wheeler and P. D. Fraser, *Microbiology-(UK)*, 2016, **162**, 1456-1467.
41 483 50. J. R. Morones, J. L. Elechiguerra, A. Camacho, K. Holt, J. B. Kouri, J. T. Ramirez
42 484 and M. J. Yacaman, *Nanotechnology*, 2005, **16**, 2346-2353.
43 485 51. D. Schnappinger and W. Hillen, *Arch. Microbiol.*, 1996, **165**, 359-369.
44 486 52. S. R. Connell, C. A. Trieber, G. P. Dinos, E. Einfeldt, D. E. Taylor and K. H.
45 487 Nierhaus, *Embo J.*, 2003, **22**, 945-953.
46 488 53. A. M. Fayaz, K. Balaji, M. Girilal, R. Yadav, P. T. Kalaichelvan and R. Venketesan,
47 489 *Nanomed.-Nanotechnol. Biol. Med.*, 2010, **6**, 103-109.
48 490 54. C. Jernberg, S. Lofmark, C. Edlund and J. K. Jansson, *Microbiology-(UK)*, 2010, **156**,
49 491 3216-3223.
50 492 55. M. Argast and C. F. Beck, *Antimicrob. Agents Chemother.*, 1984, **26**, 263-265.
51 493 56. R. W. Bundtzen, A. U. Gerber, D. L. Cohn and W. A. Craig, *Rev. Infect. Dis.*, 1981, **3**,
52 494 28-37.
53
54
55
56
57
58
59
60

- 1
2
3 495 57. K. Fuursted, A. Hjort and L. Knudsen, *J. Antimicrob. Chemother.*, 1997, **40**, 221-226.
4 496 58. F. Pomati, A. G. Netting, D. Calamari and B. A. Neilan, *Aquat. Toxicol.*, 2004, **67**,
5 497 387-396.
6 498 59. S. B. Levy, *J. Antimicrob. Chemother.*, 2002, **49**, 25-30.
7 499 60. Z. M. Xiu, J. Ma and P. J. J. Alvarez, *Environ Sci Technol*, 2011, **45**, 9003-9008.
8 500 61. R. Gurbanov, S. N. Ozek, S. Tunçer, F. Severcan and A. G. Gozen, *J. Biophotonics*,
9 501 2017, Doi: 10.1002/jbio.201700252.
10 502 62. R. Gurbanov, N. Simsek Ozek, A. G. Gozen and F. Severcan, *Anal Chem*, 2015, **87**,
11 503 9653-9661.
12 504 63. M. Kardas, A. G. Gozen and F. Severcan, *Aquat Toxicol*, 2014, **155**, 15-23.
13 505 64. S. Kjelleberg, B. A. Humphrey and K. C. Marshall, *Appl. Environ. Microbiol.*, 1983,
14 506 **46**, 978-984.

15
16 507

17
18 508
19
20
21
22
23
24
25
26
27
28
29
30
31
32
33
34
35
36
37
38
39
40
41
42
43
44
45
46
47
48
49
50
51
52
53
54
55
56
57
58
59
60

Comments:

In this study the authors applied a spectrochemical approach coupled with multivariate analysis to signature Gram-positive versus Gram-negative bacteria to characterize the underlying chemical alterations of these microorganisms in different growth phases post exposure with the antibiotic tetracycline with/without nanoparticulate silver. The manuscript covers an interesting subject that is translating real-world environmental bacteria conditions to laboratory or vice versa. This strategy can be used especially at nutrient-depleted conditions. For this reason, the impact of the presented work is very important for the development of antimicrobial strategies against pathogens.

There are some points that should be addressed to improve the manuscript.

1. I would expect more detailed microbiological experiments, probably authors performed these experiments but did not present them. I would like to see the details of the microbiological experiments. How the antimicrobial concentrations were chosen, is unclear. I recommend to perform MIC experiments for each antimicrobial. Also, CFU numbers for each condition should be provided.

Reply: Thank you for the comments; we have added more details of the experimental procedure for cultivation and exposure. Please see line 99-108. The antimicrobial concentrations were determined by their natural level reported by other's work¹⁻⁴. and our previous work of short-term exposure⁵. The CFU numbers of each exposure was 1×10^7 cells/mL and the information is added in line 101. Also, we found such low exposure was about 2-4 orders of magnitude lower than the MIC in literature review, and we thus believe the low exposure does not inhibit bacterial growth in our study. We have added relevant discussion in line 103-108.

2. Although the manuscript covers an interesting subject in a proper way, the authors claim that they developed spectrochemical tool based on ATR-FTIR spectroscopy. ATR-FTIR and chemometrics were exploited previously for bacteria characterization. Some of the previous works should be cited.

Reply: Thank you for the comments; we have added more information and discussion addressing the use of ATR-FTIR and chemometrics in previous studies. Please see line 77-87.

3. Results and discussion part might be extended definitely. Please cite more recent literature dealing with antimicrobials and/or silver salts (e.g., please see Gurbanov et al. J Biophotonics, 2017). I would expect more interesting discussion at molecular level other than microbiology textbook knowledge. Furthermore, the authors may consider to provide comparison between two different bacteria species with respect to their spectrochemical profile in the discussion part.

Reply: Thank you for your comments; we have added more discussion according to the given reference and other relevant literatures. Please see line 342-348. We have also revised Table 1 and other discussions to address the

1
2
3 comparison between two bacterial species. Please see line 193-196, 210-212,
4 320-336.
5

6
7 4. For spectral analyses part, the references for each analyzed bands should be
8 given. More extensive spectral preprocessing should be performed. The presentation
9 of band alterations is confusing and they should be discussed in a perceptible way
10 (Table 1 is confusing). Also, more details for ATR-FTIR and PCA-LDA experiment
11 procedures are needed.
12

13 **Reply:** Thank you for your comments; we have added more details and
14 references about each analyzed band. Please see line 166-170, 176-179,
15 199-210, 231-238, 246-248, 258-265.
16

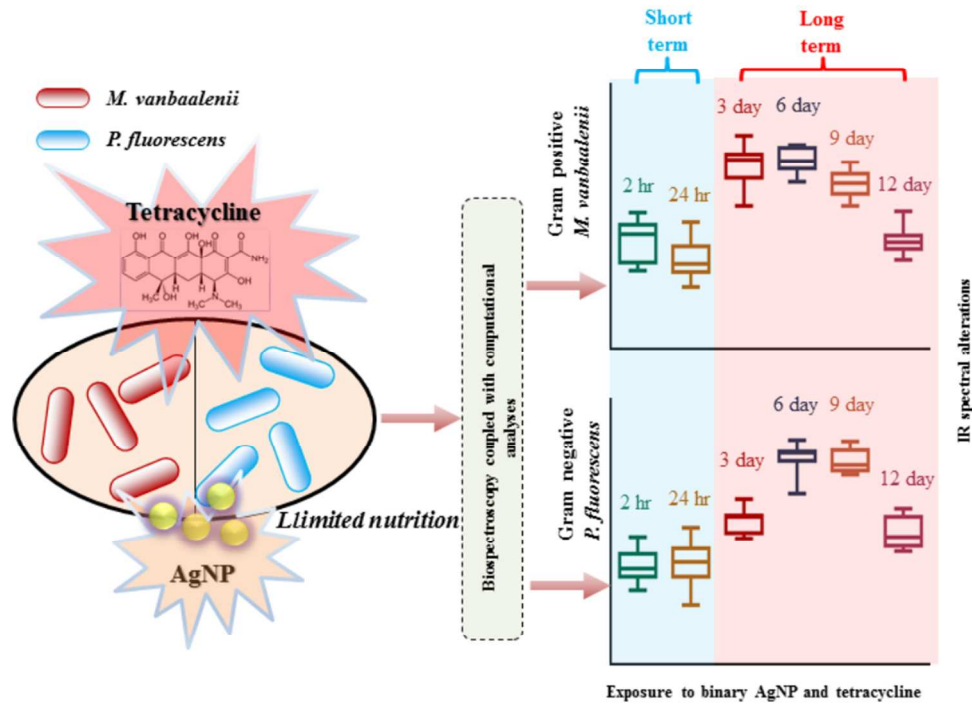
17 We have also revised the caption of Table 1 for a better expression, which
18 provides an overall summary of spectrochemical profile based on cluster
19 vector results of treatments to compare the spectrochemical profile between
20 Gram+/-ve. Please see line 193-196.
21

22
23 5. I am confused with the following sentence “The identical spectral biomarkers in
24 both Gram-positive (*M. Vanbaalenii*) and Gram-negative (*P. fluorescens*) bacteria are
25 associated with Amide I, Amide III and proteins ($\sim 1204\text{ cm}^{-1}$, $\sim 1647\text{ cm}^{-1}$) (Table 1).
26 The main changes appearing in *M. Vanbaalenii* are Amide III, proteins ($\sim 1204\text{ cm}^{-1}$,
27 $\sim 1400\text{ cm}^{-1}$), Amide I, amide II and amide III are well known protein bands. Why the
28 authors give separate protein assignment for another band as if Amide I, II and III are
29 not the protein bands, this terminology should be corrected, otherwise it will mislead
30 to researcher who are new in the area.
31

32 **Reply:** Thank you for your comments; we have corrected the misleading
33 information by deleting the confusing separate protein assignment. Please see
34 line 166-170.
35
36
37

38 References

- 39 1. R. Hirsch, T. Ternes, K. Haberer and K.-L. Kratz, *Sci Total Environ*, 1999, **225**,
40 109-118.
- 41 2. R. Hirsch, T. A. Ternes, K. Haberer, A. Mehlich, F. Ballwanz and K.-L. Kratz,
42 *Journal of Chromatography A*, 1998, **815**, 213-223.
- 43 3. G. Artiaga, K. Ramos, L. Ramos, C. Cámara and M. Gómez-Gómez, *Food*
44 *Chemistry*, 2015, **166**, 76-85.
- 45 4. T. Silva, L. R. Pokhrel, B. Dubey, T. M. Tolaymat, K. J. Maier and X. Liu, *Sci*
46 *Total Environ*, 2014, **468**, 968-976.
- 47 5. N. Jin, K. T. Semple, L. Jiang, C. Luo, D. Zhang and F. L. Martin, *Analyst*,
48 2018, **143**, 768-776.
49
50
51
52
53
54
55
56
57
58
59
60



Exposure duration and nutrient depletion strongly influence microbial responses to low-level and prolonged environmental exposures.

269x203mm (96 x 96 DPI)

1
2
3 1 **Spectrochemical determination of unique bacterial responses following long-term low-**
4
5 2 **level exposure to antimicrobials**

6
7 3 Naifu Jin^{a,b}, Kirk T Semple^a, Longfei Jiang^c, Chunling Luo^c, Francis L Martin^{d,*}, Dayi
8 4 Zhang^{a,b,*}

9
10
11 5 *^aLancaster Environment Centre, Lancaster University, Lancaster LA1 4YQ, UK*

12
13
14 6 *^bSchool of Environment, Tsinghua University, Beijing 100084, China*

15
16
17 7 *^cGuangzhou Institute of Geochemistry, Chinese Academy of Sciences, Guangzhou 510640,*
18 8 *China*

19
20
21 9 *^dSchool of Pharmacy and Biomedical Sciences, University of Central Lancashire, Preston PR1*
22 10 *2HE, UK*

23
24
25 11
26
27 12 ***Corresponding authors:**

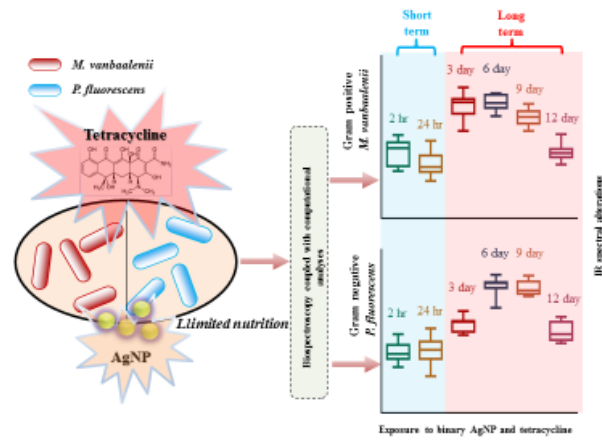
28
29 13 Francis L Martin, School of Pharmacy and Biomedical Sciences, University of Central
30 14 Lancashire, Preston PR1 2HE, UK; Email: flmartin@uclan.ac.uk

31
32
33 15 Dayi Zhang, School of Environment, Tsinghua University, Beijing 100084, China; Email:
34 16 zhangdayi@tsinghua.org.cn

35
36
37 17
38
39
40
41
42
43
44
45
46
47
48
49
50
51
52
53
54
55
56
57
58
59
60

18 ToC graphic

19



20

21

22 Abstract

23 Agents arising from engineering or pharmaceutical industries may induce significant
24 environmental impacts. Particularly, antimicrobials not only act as efficient eliminators of
25 certain microbes but also facilitate the propagation of organisms with antimicrobial
26 resistance, raising critical health issues, *e.g.*, the bloom of multidrug-resistant bacteria.
27 Although many investigations have examined microbial responses to antimicrobials and
28 characterized relevant mechanisms, they have focused mainly on high-level and short-term
29 exposures, instead of simulating real-world scenarios in which the antimicrobial exposure is
30 at a low-level for long periods. Herein, we developed a spectrochemical tool, attenuated total
31 reflection Fourier-transform infrared (ATR-FTIR) spectroscopy, as a high-throughput and
32 nondestructive approach to interrogate the long-term effects of low-level antimicrobial
33 exposure in bacterial cells. Post-exposure to nanoparticulate silver (AgNP), tetracycline or
34 their mixtures for 12 days, Gram-positive (*Mycobacterium vanbaalenii* PYR-1) and Gram-
35 negative (*Pseudomonas fluorescens*) bacteria exhibited distinct IR spectral alterations.
36 Multivariate analysis coupled with multivariate regression tree (MRT) indicates nutrient
37 depletion and exposure time as the primary factors in bacterial behaviour, followed by
38 exposure category and bacterial type. Nutrient depletion and starvation during long-term
39 exposure drives bacterial cells into a dormant state or to exhibit additional cellular
40 components (*e.g.*, fatty acids) in response to antimicrobials, consequently causing a broader
41 range of spectral alterations compared to short-term exposure. This work is the first report
42 highlighting the more important roles of exposure duration and nutrient depletion, instead of
43 treatment regimen of antimicrobial, on microbial responses to low-level and prolonged
44 environmental exposures.

45

1. Introduction

Environmental exposure to antimicrobials is a critical issue for both human and microbial communities. Antibiotics are currently ranked as the third most commonly prescribed drugs¹. In human and veterinary medicine there is abuse of antibiotics, especially for keeping animals healthy at a sub-therapeutic level²⁻⁹. The primary sink for such antibiotic usage is the environment, *e.g.*, waters and soils, *via* various pathways post-excretion^{2, 3 4, 6}. Another group of frequently-used antimicrobial agents is silver-associated entities. Notably, unlike silver ion or salts whose antimicrobial effects are well-studied, the mechanisms of nanoparticulate silver (AgNP) activity remain unclear. However, AgNP is widely exploited for its antibacterial activity, in clothing, food containers, wound dressings, ointments, implant coatings, and ultrafiltration membranes for water purification¹⁰⁻¹⁴. Developing a reliable approach to interrogate microbial responses to antimicrobials is therefore a matter of urgency, contributing to better understanding of the mechanisms and impacts of antimicrobial agents on environmental microbes¹⁵.

A major issue is the translation from laboratory culture to the real-world scenario of bacteria living in their natural habitats. In contrast to most laboratory culture conditions, *e.g.*, nutrient rich broth, free-living bacteria commonly face nutrient depletion or even more prohibitive circumstances¹⁶. For instance, cells inhabiting biofilm may be exposed to different concentrations of nutrients, metabolites or environmental stimuli (*e.g.*, temperature, pH, oxygen, etc.)¹⁷⁻²¹ across the biofilm matrix and local microenvironment, leading to heterogeneous growth rates and behaviours amongst the cell populations^{22, 23}. Amongst these, a small proportion might differentiate into a highly protected phenotypic state and coexist with neighbouring populations that are antibiotic sensitive, resulting from inherent strain differences and adaptation to relatively low concentrations of exposure^{16, 22, 23}. Moreover, although regulatory agencies and pharmaceutical administration generally employs high doses of antimicrobials in *in-vivo* and *in-vitro* trials to ensure the safety of test chemicals, residual exposure is typically associated with extremely low-levels in the physical environment; this raises question as to whether high-concentrations of exposure represent the real-world outcomes²⁴⁻²⁹. Thus, research on prolonged low-level exposures of antimicrobials is required in order to shed deeper insights into microbial responses to antimicrobials in the real-world environment¹⁵.

1
2
3 77 Despite recently developed molecular techniques towards targeting microbial
4
5 78 phenotypes, such approaches to identify minor or pre-stage phenotypic alterations induced by
6
7 79 low-level exposure remain limited³⁰⁻³³. Meanwhile, other confounding factors (*e.g.*, microbial
8
9 80 species, growth phase, exposure time, etc.) may also influence test results^{16, 31, 34}. In 1991,
10
11 81 Fourier-transform infrared (FTIR) spectroscopy was innovatively introduced as a sensitive
12
13 82 and rapid screening tool for the characterization, classification and identification of
14
15 83 microorganisms¹⁶. Since then, the emerging application of spectrochemical techniques with
16
17 84 computational analysis as an inter-discipline approach shows promising feasibility in
18
19 85 microbiology and cytology³⁰⁻³⁶. In the last decade, FTIR spectroscopy plus chemometrics has
20
21 86 been exploited broadly for identifying microbial identities, physiologies, activities and related
22
23 87 functions^{16, 30, 31, 33, 34, 37, 38}. This technical combination provides a major advantage in terms
24
25 88 of being high-throughput, label-free and cost-effective in application³⁰, allowing one to
26
27 89 interrogate biological samples *via* a nondestructive and nonintrusive manner, which has great
28
29 90 potential in monitoring real-world scenarios^{30-32, 34}.

30
31 91 The current study applied attenuated total reflection FTIR (ATR-FTIR) microscopy
32
33 92 coupled with multivariate analysis to investigate bacterial responses to prolonged low-level
34
35 93 exposures of AgNP and tetracycline under nutrient depletion conditions. Compared to short-
36
37 94 term exposure, we found that length of exposure plays a more important role than treatment
38
39 95 with antimicrobial reagents or bacterial type, further uncovering key influential factors of
40
41 96 bacterial responses to antimicrobials during cell growth associated with nutrient depletion.

39 97 **2. Methodology**

41 98 *2.1 Cell strains and sample preparation*

43 99 The two bacterial strains used in this study were *Mycobacterium vanbaalenii* PYR-1 (Gram-
44
45 100 positive) and *Pseudomonas fluorescens* (Gram-negative). They were both grown in minimal
46
47 101 medium with 20 mM sodium succinate, undertaken in a dark rotary shaker at 150 rpm and the
48
49 102 culture temperature was 30±2°C. After centrifugation and washing with sterile water, cell
50
51 103 pellets were diluted in fresh minimal medium with 20 mM sodium succinate and cultivated
52
53 104 for about 2 h until they reached the early log-phase (CFU=1×10⁷ cells/mL). The four
54
55 105 treatments included non-exposure negative control (CK), 4 µg/L of AgNP, 1 µg/L of
56
57 106 tetracycline, and a mixture with 4 µg/L of AgNP and 1 µg/L of tetracycline (Binary). The
58
59 107 concentrations of AgNP and tetracycline were selected according to their previous reported
60
108 level in natural environment to mimic the low-level exposure in real-world scenario³⁸. They

1
2
3 109 are about 2-4 orders of magnitude lower than the minimum inhibitory concentration (MIC) of
4 110 AgNP (1 to 10 mg/L)^{39, 40} and tetracycline (1 to >30 mg/L)^{41, 42}, and therefore do not inhibit
5
6 111 bacterial growth. The samples of short-term exposure were taken after 2 h (late log-phase, T₀)
7
8 112 and 48 h (T₁), respectively. To create a nutrient-depletion condition for long-term exposure,
9
10 113 the cells were cultivated in 10-times diluted minimal medium and the culture medium was
11
12 114 refreshed every 72 h. The samples were collected at 3 (T₂), 6 (T₃), 9 (T₄) and 12 (T₅) days.
13
14 115 The collected cells were then harvested by centrifugation at 4000 rcf for 5 min, washed three
15
16 116 times with sterile deionized water, and finally fixed with 70% ethanol to prevent further
17
18 117 exposure.

19 118 2.2 Spectrochemical analysis

21 119 The prepared samples (minimal amount > 5 µL) were then applied onto Low-E slides and dried
22
23 120 for analysis by ATR-FTIR spectroscopy. A Bruker TENSOR 27 FTIR spectrometer (Bruker
24
25 121 Optics Ltd., UK) with a Helios ATR attachment containing a diamond internal reflection
26
27 122 element (IRE) was applied to acquire IR spectra. The data were attained at a resolution of 3.84
28
29 123 cm⁻¹, 2.2 kHz mirror velocity and 32 co-additions. The instrument parameters were set at 32
30
31 124 scans and 16 cm⁻¹ resolution. To collect the data, a total of 30 individual spectral measurements
32
33 125 were taken randomly from each sample using the aid of the ATR magnification-limited
34
35 126 viewfinder camera. Prior to analysing each new specimen, the crystal was cleaned using
36
37 127 deionized water and a background reading was taken.

38 128 2.3 Multivariate analysis and statistics

40 129 All the initial data generated from ATR-FTIR spectroscopy were analysed using MATLAB
41
42 130 R2011a (*TheMathsWorks, Natick, MA, USA*) coupled with the IRootLab toolbox
43
44 131 (<http://irootlab.googlecode.com>)⁴³. The acquired IR spectra were merged and cut to the
45
46 132 biochemical-cell fingerprint region (1800-900 cm⁻¹). Then a rubber-band baseline correction
47
48 133 was applied to remove any slopes in this area. The data were then normalized to Amide I (1650
49
50 134 cm⁻¹) and the means were centered allowing alignment of the different spectra for comparison.

51 135 Principal component analysis-linear discriminant analysis (PCA-LDA) was applied
52
53 136 after data pre-processing to reduce the number of spectra to 10 uncorrelated principal
54
55 137 components (PCs), which account for >99% of the total variance. LDA is a supervised
56
57 138 technique coupled with PCA in order to maximize interclass and minimize intraclass variance^{30,}
58
59 139 ^{31, 44}. Cross-calculation was subsequently performed to mitigate risks resulting from LDA
60
140 overfitting⁴⁵. The PCA-LDA loadings using (*n*-1) samples (*n* = number of samples in dataset)

1
2
3 141 was trained *via* leave-one-out cross-validation and then calculated the scores of the rest sample.
4
5 142 This process was performed for all scores within the test.
6

7 143 PCA-LDA cluster vectors are pseudo-spectra highlighting the key biochemical
8 alterations of each group in the dataset³⁵, which allows one to simplify the identification of
9 144 discriminating differences amongst groups. The centre of the control cluster itself is moved to
10 145 the origin of the PCA-LDA factor space. The extent of peak deviation away from the origin of
11 146 the factor space then occurs according to the centre of each corresponding agent-induced
12 147 cluster, proportional to the discriminating extent of biochemical differences^{31, 45}. Cluster
13 148 vectors plots were also applied to indicate the most prominent six significant peaks.
14 149
15
16
17
18
19

20 150 Multivariate regression trees (MRT) were used to analyse the influence of bacterial type,
21 151 exposure time and exposure category on biospectral alterations using the R package “mvpart”.
22 152 Herein, Gram-positive (*M. vanbaalenii*) and Gram-negative (*P. fluorescens*) strains were
23 153 assigned as 1 and 0. The exposure of AgNP, tetracycline and their mixtures were assigned as
24 154 1, 2 and 3, respectively. The samples collected at different time points (T₀, T₁, T₂, T₃, T₄ and
25 155 T₅) were assigned to 1, 2, 3, 4, 5 and 6, respectively.
26
27
28
29
30

31 156 One-way analysis of variance (ANOVA) with Tukey’s post-hoc test/or *t*-test was
32 157 employed to test the differences between treatments. All statistical analyses were carried out
33 158 in GraphPad Prism 6.
34
35
36

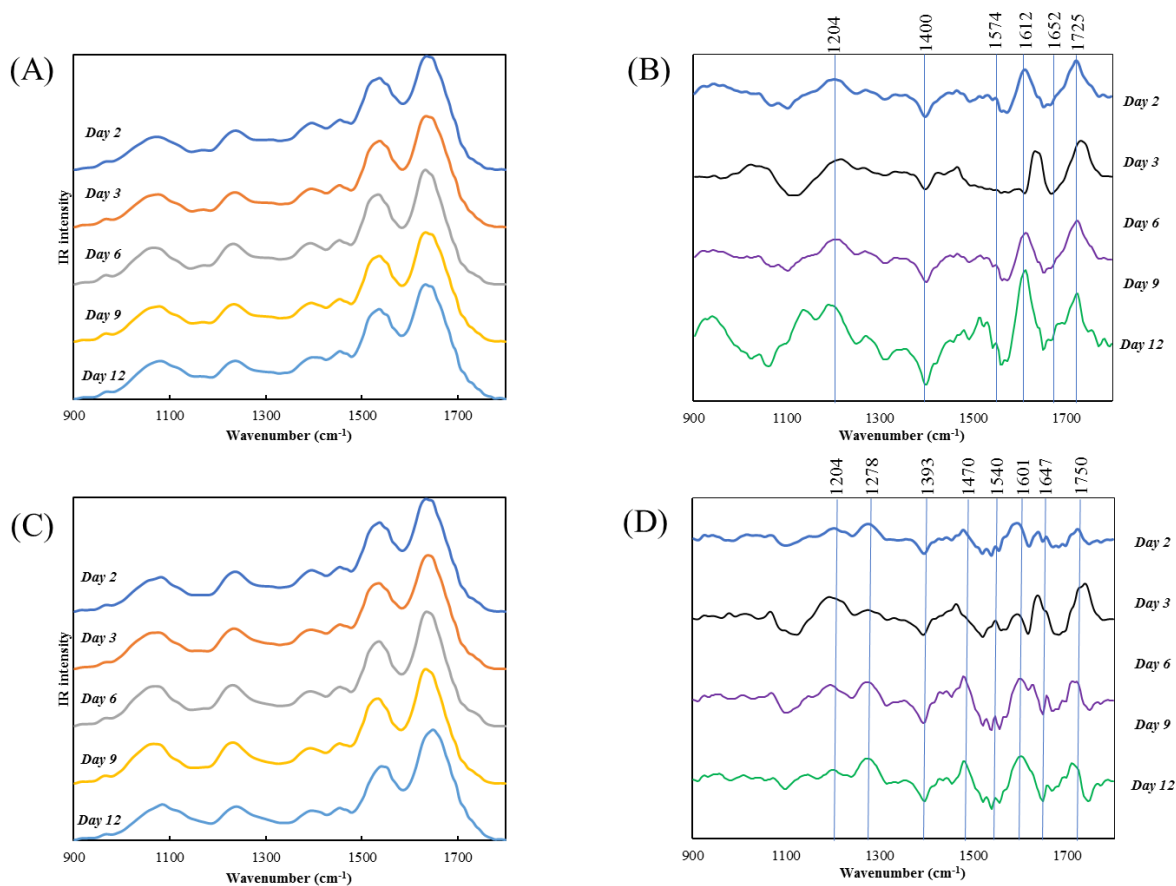
37 159 **3. Results and discussion**

38 160 *3.1 Growth-dependent spectrochemical alterations*

39 161 Throughout the study, a spectral class mean for the bacterial control group has been derived,
40 162 which generates an average spectrum based on all raw data from the same group. However,
41 163 minor variability is visualised from the class mean data directly between groups at different
42 164 time points (Figure 1A and 1B). Although previous studies suggest that bacteria with limited
43 165 nutrients are more likely to enter a dormant state waiting suitable growth conditions^{46, 47}, the
44 166 spectral alterations induced by nutrient depletion are limited. Therefore, a further cluster
45 167 vectors analysis is applied to highlight the minor alterations derived from nutrient depletion
46 168 (Figure 1C and 1D). The identical spectral biomarkers in both Gram-positive (*M.*
47 169 *Vanbaalenii*) and Gram-negative (*P. fluorescens*) bacteria are associated with Amide I,
48 170 Amide III (~1204 cm⁻¹, ~1647 cm⁻¹)^{30, 33} (Table 1). The main changes appearing in *M.*
49 171 *Vanbaalenii* are Amide III, (~1204 cm⁻¹, ~1400 cm⁻¹), C=N adenine (~1574 cm⁻¹), Amide I
50
51
52
53
54
55
56
57
58
59
60

1
2
3 172 (~1652 cm⁻¹), and C=O band (~1725 cm⁻¹)^{33, 48}. Of these, the amino acid-associated
4
5 173 alterations possibly contributing to nucleotide metabolism, which is important for cellular
6
7 174 catabolism are significant. Along with long-term starvation and oxygen depletion, decreasing
8
9 175 amounts of nucleotides are associated with reduced cell activities and replication compared to
10
11 176 log-phase. Furthermore, alterations in other cellular components (*e.g.*, proteins) might be
12
13 177 mainly responsible for cell wall maintenance, based on previous study⁴⁹.

14 178 The specific spectrochemical alterations of *P. fluorescens* include Amide III (~1278
15
16 179 cm⁻¹), CH₂ bending of the methylene chains in lipids (~1470 cm⁻¹), protein Amide II
17
18 180 absorption (~1540 cm⁻¹), C=N cytosine (~1601 cm⁻¹), ν (C=C) lipids, and fatty acids (~1750
19
20 181 cm⁻¹)^{34, 48}. Accordingly, more lipid alterations under nutrient depletion conditions are found
21
22 182 in Gram-negative *P. fluorescens* versus Gram-positive *M. vanbaalenii* owing to their
23
24 183 differing cell wall structures. There is only a thin peptidoglycan layer (~2-3 nm) between the
25
26 184 cytoplasmic and outer membrane in Gram-negative bacteria, whereas the outer membrane in
27
28 185 Gram-positive bacteria is a thick peptidoglycan layer of 30 nm with no other additional
29
30 186 structure⁵⁰. The attributes of membrane structure may explain the distinct spectrochemical
31
32 187 alterations between *P. fluorescens* and *M. vanbaalenii* under nutrient depletion, which might
33
34 188 lead to different responses towards long-term exposure of antimicrobials.
35
36
37
38
39
40
41
42
43
44
45
46
47
48
49
50
51
52
53
54
55
56
57
58
59
60



189

190 **Figure 1.** Spectrochemical alterations with length of culture. Infrared spectra of *M.*
191 *vanbaalenii* (A) and *P. fluorescens* (C) from control group. Cluster vectors plots of *M.*
192 *vanbaalenii* (B) and *P. fluorescens* (D) from control group, indicating significant
193 wavenumbers contributing to segregating spectral alterations that develop with increasing
194 culture time.

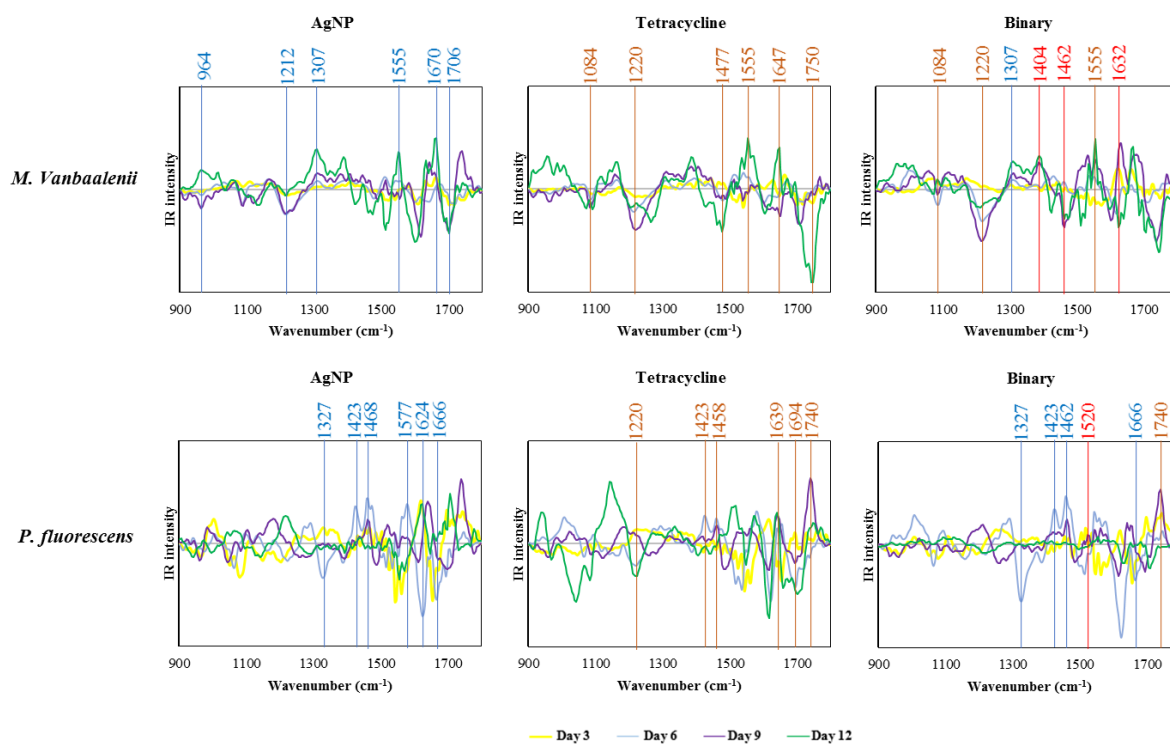
1
2
3 **Table 1.** Spectrochemical profile regarding the significant spectral biomarkers peaks derived from cluster vectors of *M. vanbaalenii* (Gram-
4 positive) and *P. fluorescens* (Gram-negative) post-exposure to AgNP, tetracycline and their mixtures. Red dots represent identical biomarkers for
5 196 both Gram-positive and Gram-negative bacteria, and green and blue dots indicate biomarkers appear only in Gram-positive or Gram-negative
6 197 bacteria, respectively.
7
8
9

Wavenumber (cm ⁻¹)	Annotation	Gram-positive				Gram-negative			
		Growth	AgNP	Tetracycline	Binary	Growth	AgNP	Tetracycline	Binary
~ 964	C-C, C-O deoxyribose	-	●	-	-	-	-	-	-
~ 1084	DNA	-	-	●	●	-	-	-	-
~ 1204	Amide III	●	-	-	-	●	-	-	-
~ 1212	Phosphate	-	●	-	-	-	-	-	-
~ 1220	PO ₂ ⁻ stretching in RNA and DNA	-	-	●	●	-	-	●	-
~ 1278	Amide III	-	-	-	-	●	-	-	-
~ 1307	Amide III	-	●	-	●	-	-	-	-
~ 1327	Stretching C-N thymine, adenine	-	-	-	-	-	●	-	●
~ 1393		-	-	-	-	●	-	-	-
~ 1400		●	-	-	-	-	-	-	-
~ 1404	CH ₃ asymmetric deformation	-	-	-	●	-	-	-	-
~ 1423		-	-	-	-	-	●	●	●
~ 1458	Lipids and proteins	-	-	-	-	-	-	●	-
~ 1462		-	-	-	●	-	-	-	●
~ 1468		-	-	-	-	-	●	-	-
~ 1470	CH ₂ bending of the methylene chains in lipids	-	-	-	-	●	-	-	-
~ 1477		-	-	●	-	-	-	-	-
~ 1520	Amide II	-	-	-	-	-	-	-	●
~ 1540	Protein amide II absorption	-	-	-	-	●	-	-	-
~ 1555	Ring base	-	●	●	●	-	-	-	-
~ 1574	C=N adenine	●	-	-	-	-	-	-	-

1									
2									
3	~ 1577	C-C stretch	-	-	-	-	-	●	-
4	~ 1601	C=N cytosine	-	-	-	-	●	-	-
5	~ 1612		●	-	-	-	-	-	-
6	~ 1624		-	-	-	-	-	●	-
7	~ 1632	C-C stretch	-	-	-	●	-	-	-
8	~ 1639	Amide	-	-	-	-	-	-	●
9	~ 1647	Amide I	-	-	●	-	●	-	-
10	~ 1652	Amide I	●	-	-	-	-	-	-
11	~ 1666	C=O stretching vibration of pyrimidine base	-	-	-	-	-	●	●
12	~ 1670	Amide I	-	●	-	-	-	-	-
13	~ 1694	Proteins	-	-	-	-	-	-	●
14	~ 1706	C=O thymine	-	●	-	-	-	-	-
15	~ 1725	C=O band	●	-	-	-	-	-	-
16	~ 1740	C=O, lipids	-	-	-	-	-	-	●
17	~ 1750	v(C=C) lipids, fatty acids	-	-	●	-	●	-	●
18									
19									
20									
21									
22	199								
23									
24									
25									
26									
27									
28									
29									
30									
31									
32									
33									
34									
35									
36									
37									
38									
39									
40									
41									
42									
43									
44									
45									
46									

200 3.2 Spectrochemical alterations with long-term AgNP/tetracycline exposure

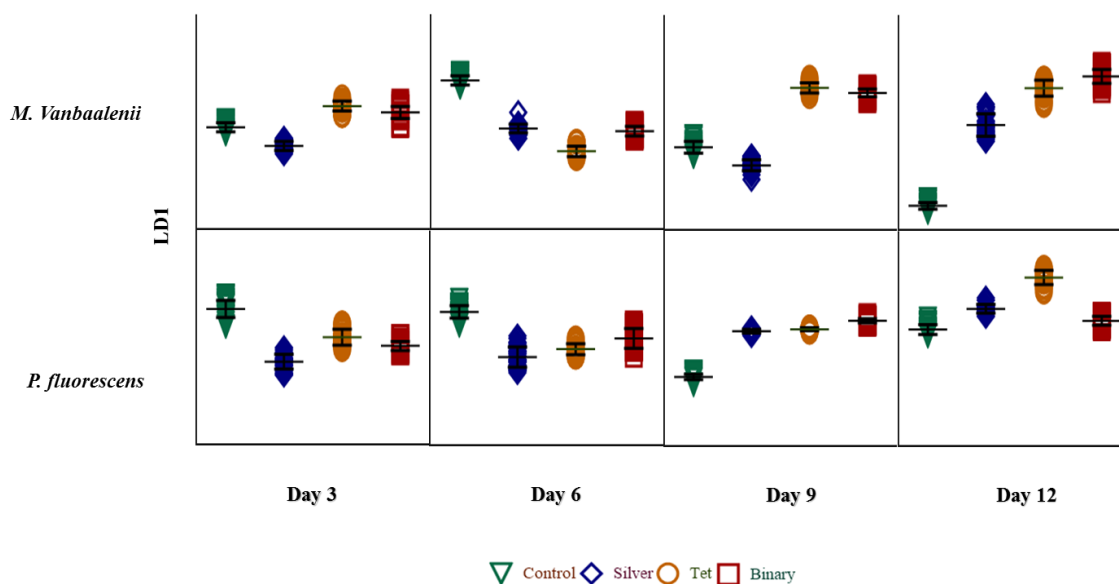
201 To identify exposure-induced alterations, the spectral data of each treatment group are
202 compared with the control group at the same time point, eliminating the impacts of cell
203 growth and nutrient depletion (Figure 2). In Gram-positive *M. Vanbaalenii*, the AgNP-
204 induced alterations are C-C, C-O deoxyribose ($\sim 964\text{ cm}^{-1}$), phosphate ($\sim 1212\text{ cm}^{-1}$), Amide
205 III ($\sim 1307\text{ cm}^{-1}$), ring base ($\sim 1555\text{ cm}^{-1}$), Amide I ($\sim 1670\text{ cm}^{-1}$), and C=O thymine (~ 1706
206 cm^{-1})^{30, 33, 38}. Post-exposure to tetracycline, the representative peaks are DNA ($\sim 1084\text{ cm}^{-1}$),
207 PO_2^- stretching in RNA and DNA ($\sim 1220\text{ cm}^{-1}$), ring base ($\sim 1555\text{ cm}^{-1}$), Amide I (~ 1647
208 cm^{-1}), lipids, and fatty acids ($\sim 1750\text{ cm}^{-1}$)^{33, 38, 48}. With the binary exposure, the alterations
209 are different from individual exposures, and the specific spectral biomarkers are DNA (~ 1084
210 cm^{-1}), PO_2^- stretching in RNA and DNA ($\sim 1220\text{ cm}^{-1}$), Amide III ($\sim 1307\text{ cm}^{-1}$), CH_3
211 asymmetric deformation ($\sim 1404\text{ cm}^{-1}$, $\sim 1462\text{ cm}^{-1}$), ring base ($\sim 1555\text{ cm}^{-1}$), and C-C stretch
212 ($\sim 1632\text{ cm}^{-1}$)^{38, 48}. It is worth mentioning that the binary effects of AgNP and tetracycline on
213 *M. vanbaalenii* spectra are mainly driven by tetracycline as more identical discriminating
214 peaks are observed between these two groups (Table 1). To evaluate the impacts of each
215 exposure, PCA-LDA score plots were generated and illustrate the increasing segregation
216 between groups with increasing exposure time (from day 3 to day 12, Figure 3). Particularly,
217 the biochemical distances of tetracycline and binary groups are co-located, apparently
218 separated from the control group and markedly on day 12. However, the AgNP-treated
219 groups only show slight shifting of biochemical differences compared to the control group.
220 This result is consistent with cluster vectors analysis that the binary-exposure effects in *M.*
221 *vanbaalenii* are closer to tetracycline alone than AgNP.



222

223 **Figure 2.** Cluster vectors plots after PCA-LDA, indicating significant wavenumbers for the
 224 segregation of *M. vanbaalenii* and *P. fluorescens* following long-term exposure (day 3 to day
 225 12) to AgNP, tetracycline or their mixtures.

226



227

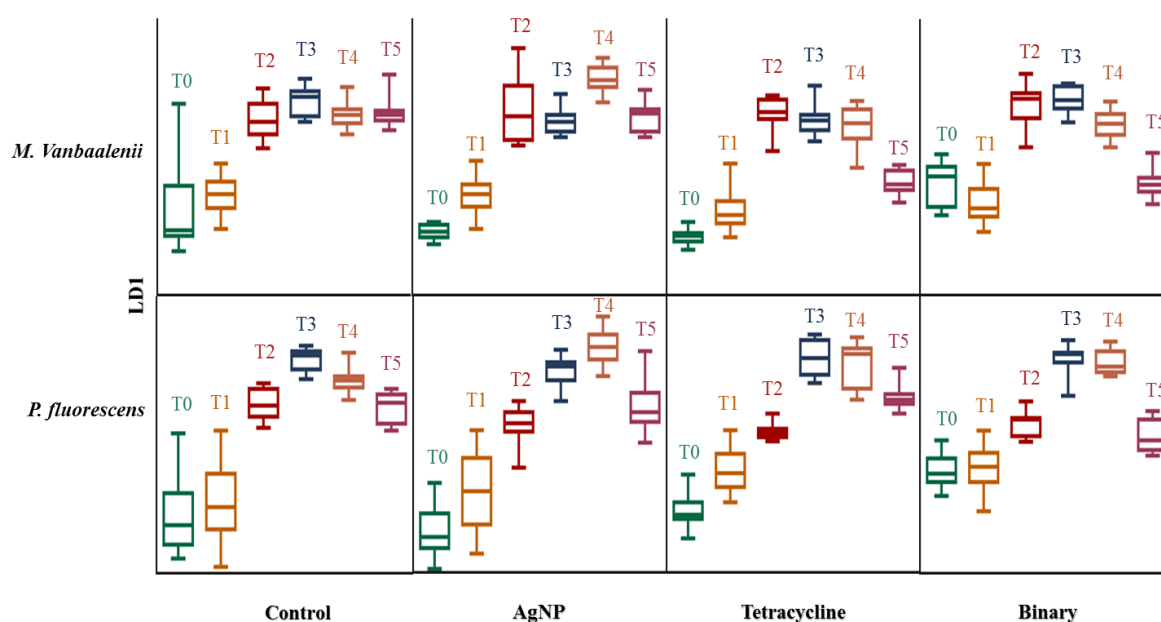
228 **Figure 3.** PCA-LDA score plots for the biospectral alteration of *M. vanbaalenii* and *P.*
 229 *fluorescens* following long-term exposure (day 3 to day 12) to AgNP, tetracycline or their
 230 mixtures.

1
2
3 231 In Gram-negative *P. fluorescens*, all the exposure groups are clearly separated from the
4 control group in the PCA-LDA score plots (Figure 3), and there is no significant difference
5 232 between each treatment. The AgNP-induced alterations include stretching C-N thymine,
6 233 adenine ($\sim 1327\text{ cm}^{-1}$), lipids and proteins ($\sim 1458\text{ cm}^{-1}$), C-C stretch ($\sim 1577\text{ cm}^{-1}$), (~ 1624
7 234 cm^{-1}), and C=O stretching vibration of pyrimidine base ($\sim 1666\text{ cm}^{-1}$)⁴⁸. The tetracycline-
8 235 induced peaks are DNA ($\sim 1220\text{ cm}^{-1}$); ($\sim 1423\text{ cm}^{-1}$), collagen ($\sim 1458\text{ cm}^{-1}$), Amide I (~ 1639
9 236 cm^{-1} , $\sim 1694\text{ cm}^{-1}$), and C=O lipids ($\sim 1740\text{ cm}^{-1}$)^{38, 48}. Generally, outer cellular components
10 237 are widely affected by both AgNP and tetracycline, including Amides I/II and proteins
11 238 ($\sim 1307\text{ cm}^{-1}$, $\sim 1647\text{ cm}^{-1}$, $1639\text{ -}1694\text{ cm}^{-1}$), and lipids and/or fatty acids (1750 cm^{-1} , 1458
12 239 cm^{-1} , 1740 cm^{-1})^{30, 33, 38, 48}, indicating that the cell membrane is the primary reactive target
13 240 associated with both antimicrobials which penetrate bacterial cells *via* passive diffusion and
14 241 inhibit bacterial growth by perturbing protein synthesis or altering membrane structure⁵¹.
15 242 Additionally, more inner cellular components are identified to be associated with tetracycline
16 243 exposure than AgNP, *e.g.*, inherent DNA and RNA, possibly due to the antibiotic mechanism
17 244 of tetracycline which blocks the elongation cycle by preventing incoming aminoacyl-tRNA
18 245 (aa-tRNA) from binding to the ribosomal A-site and inhibiting protein synthesis⁵². Different
19 246 from Gram-positive strains, AgNP-induced alterations contribute predominantly to the binary
20 247 effects in *P. fluorescens*, *i.e.*, stretching C-N thymine, adenine ($\sim 1327\text{ cm}^{-1}$, $\sim 1423\text{ cm}^{-1}$,
21 248 $\sim 1462\text{ cm}^{-1}$), Amide II ($\sim 1520\text{ cm}^{-1}$), C=O stretching vibration of pyrimidine base (~ 1666
22 249 cm^{-1}), and C=O lipids ($\sim 1740\text{ cm}^{-1}$)^{31, 34}. These findings imply the antimicrobial synergism
23 250 of AgNP and tetracycline. A previous study suggests that antibiotics' efficacy against
24 251 microbes may increase in the presence of AgNP because of the bonding reaction between
25 252 antibiotics and nanofillers, owing to the chelating reaction of hydroxyl and amide groups in
26 253 antibiotic molecules with AgNP⁵³.
27 254

255 3.3 Impacts of exposure time on spectrochemical alterations

256 Although short-term impacts by antimicrobials on bacteria is obvious and well-studied, their
257 consequences may last for extended periods and remain unknown⁵⁴. To unravel such long-
258 term exposure effects, we measured the biospectral alterations at different time points, and
259 found distinguishing biomarkers post-exposure to antimicrobials between short-term *versus*
260 long-term treatments (Figure 4). Generally, in short-term exposure (≤ 3 days), spectral
261 changes are associated with components from cell membranes wherein most antimicrobial-
262 induced alterations occur in both strains, including glycogen ($\sim 1022\text{ cm}^{-1}$), symmetric
263 phosphate stretching vibrations ($\nu_s\text{PO}_2^-$; $\sim 1088\text{ cm}^{-1}$, 1092 cm^{-1}), carbohydrates (~ 1165

264 cm^{-1}), protein phosphorylation ($\sim 964 \text{ cm}^{-1}$), Amide I ($\sim 1609 \text{ cm}^{-1}$, 1612 cm^{-1} , 1659 cm^{-1} ,
 265 $\sim 1670 \text{ cm}^{-1}$), Amide III ($\sim 1269 \text{ cm}^{-1}$), COO- symmetric stretching vibrations of fatty acids
 266 and amino acid ($\sim 1408 \text{ cm}^{-1}$), proteins ($\sim 1485 \text{ cm}^{-1}$, $\sim 1550 \text{ cm}^{-1}$, $\sim 1650 \text{ cm}^{-1}$), and lipids
 267 ($\sim 1701 \text{ cm}^{-1}$, $1705\text{-}1750 \text{ cm}^{-1}$)^{30, 32, 38, 48}. Besides external cellular components, some
 268 inherent elements are significantly influenced in long-term exposure (>3 days). For instance,
 269 long-term tetracycline-induced alterations in *P. fluorescens* include RNA and DNA (e.g.,
 270 $\sim 1220 \text{ cm}^{-1}$, $\sim 1423 \text{ cm}^{-1}$). Compared to prolonged exposure, short exposure induces minimal
 271 alterations, possibly owing to bacteria undergoing pre-stage reactions against antimicrobials.
 272 During extended exposure periods, the more obvious biospectral alterations might be
 273 explained by increasing tetracycline accumulation *via* penetration and stronger antibiotic
 274 effects, which prevent RNA binding to the ribosomal A-site and protein synthesis⁵², and
 275 further inhibit RNA/DNA synthesis and duplication⁵⁵. Another explanation is the post-
 276 antibiotic effect (PAE) or lag of bacterial regrowth induced by long-term antimicrobial
 277 exposure, driving bacterial entry into a growth suppression state^{56, 57}.



278

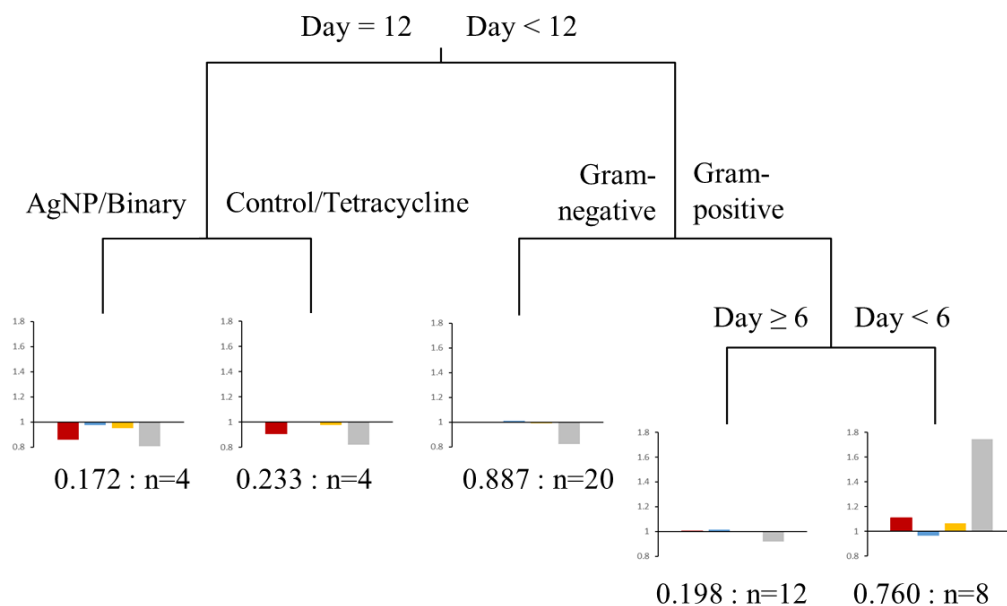
279 **Figure 4.** PCA-LDA score plots of the biospectral alteration of *M. vanbaalenii* and *P.*
 280 *fluorescens* in both short-term and long-term exposure to AgNP, tetracycline and their
 281 mixtures. T₀, T₁, T₂, T₃, T₄ and T₅ represent exposure time of 2 h, 2 days, 3 days, 6 days, 9
 282 days and 12 days, respectively.

283

284 3.4 Influential factors determining bacterial long-term responses to antimicrobials

285 Although distinct impacts of different antimicrobials on bacteria have been well-documented,
286 many variables including intrinsic and external factors may alter such influences in real-
287 world scenarios. In the present study, we evaluated bacterial type, exposure category,
288 exposure time and nutrient depletion, but which factor is the most dominating remains
289 unclear. To answer this question, a multivariate regression trees (MRT) analysis based on
290 isolated discriminating biomarkers is conducted to quantify the impacts of these four factors
291 on spectral alterations. MRT visualizes these influencing factors on spectral variations in a
292 tree with four splits based on exposure time, exposure category, bacterial type and nutrient
293 depletion, explaining 63.7% of the total spectral variance (Figure 5). Level of influence is
294 ranked as exposure time > exposure type > bacterial type = nutrient depletion. Exposure time
295 accounts for 17.8% of the total variance, with the first split separating the group of 12-day
296 exposure owing to the relatively lower intensities of DNA. In the 12-day exposure group,
297 exposure category explains 16.1% of the variance and splits spectra into two groups of
298 control/tetracycline and AgNP/binary, mainly based on DNA spectral biomarkers. The group
299 of exposure <12 days is further split by bacterial type, accounting for 14.9% of the total
300 variance and attributed to differences in DNA, phospholipid-derived fatty acids and proteins.
301 The final split representing nutrient depletion separates the groups of 6-9 day and 0-3 day for
302 Gram-positive bacteria (*M. vanbaalenii*, 14.9%), owing to higher cellular activities reflected
303 by significant variations in DNA, phospholipid-derived fatty acids and proteins.

304 The MRT results are consistent with PCA-LDA score plots (Figure 4). The spectral
305 distances of *P. fluorescens*, for instance, are similar regardless of exposure categories from
306 day 9 due to cell regeneration against the exposure and exhibiting resistance to
307 antimicrobials⁴⁶. A prior study reported that long-term exposure (5 days) to 1 µg/L of
308 tetracycline shows no apparent effect on cyanobacterial cells due to their natural variability in
309 tetracycline resistance⁵⁸. It might explain the closer distance between groups of control and
310 tetracycline. Moreover, the distinct behaviours of *M. vanbaalenii* and *P. fluorescens* upon
311 starvation can explain the fourth split in MRT, *i.e.*, *M. vanbaalenii* enters a replicative state
312 after 6-day exposure to adapt to conditions of insufficient nutrients, whereas *P. fluorescens*
313 appears more susceptible to nutrient depletion and starts regrowth. Evidence can be found
314 from the additional cellular components produced in Gram-negative *P. fluorescens*, *e.g.*, fatty
315 acids (~1750 cm⁻¹), as their predominant energy to survive⁴⁶.



Error: 0.364 CV Error: 0.572 SE: 0.119

316

317 **Figure 5.** Multivariate regression tree (MRT) analysis of environmental variables explaining
 318 discriminating biomarkers. The scale of the sub-figures reflects the alteration degree (number
 319 one represents the average level). Red bars represent biomarkers assigned to DNA; blue bars
 320 represent biomarkers associated with proteins; yellow bars represent biomarkers assigned to
 321 phospholipid-derived fatty acids; and, grey bars represent other cellular components.

322

323 Moreover, bacterial type may also have impacts on the consequences posed by antimicrobials
 324 since bacteria differ in their cellular structures. Antimicrobials acting as both efficient
 325 eliminators to microbes and selective agents help to propagate organisms with resistance
 326 ability⁵⁹. Herein, we found discriminating alterations between Gram-positive and Gram-
 327 negative strains within the same exposure treatment. All the treatments exhibit distinct
 328 alterations in Gram-positive *M. vanbaalenii* under nutrient depletion conditions (Day 3 to
 329 Day 12), although AgNP generates very limited impact as compared to tetracycline or binary
 330 exposure groups; these are not observed in *P. fluorescens*. The results from PCA-LDA scores
 331 plots (Figure 3) and MRT (Figure 5) also show induced alterations in *M. vanbaalenii* are
 332 significant compared to *P. fluorescens*. Furthermore, after long-term exposure (12 days),

1
2
3 333 Gram-negative *P. fluorescens* exhibit a broad range of spectral alterations assigned to lipids
4 334 and/or fatty acid (*e.g.*, 1458 cm⁻¹, 1740 cm⁻¹), which are absent in Gram-positive *M.*
5
6 335 *vanbaalenii*, mainly attributed to their different cell wall structures. The rigidity and extended
7
8 336 cross-linking may reduce the target sites in cell membranes for environmental exposures and
9
10 337 afford further protection to cells from antimicrobial penetration^{12, 53}. It implies that cell
11
12 338 membranes of Gram-negative bacteria are more likely to be influenced compared to Gram-
13
14 339 positive bacteria under certain antibacterial treatments (*e.g.*, AgNP)^{12, 50, 60}. Past studies report
15
16 340 the oxidation of smaller AgNPs (1-10 nm) by intercellular reactive oxygen species (ROS) in
17
18 341 Gram-negative bacteria, resulting in the release of silver ions during AgNP penetration
19
20 342 through the cell membrane and entrance into the cytoplasm⁶⁰. These silver ions could be
21
22 343 further transferred to other Gram-negative bacterial cells, the membrane and cytoplasm which
23
24 344 contain many sulfur-containing proteins for the released Ag⁺ to bind to and inactivate^{50, 60}.
25
26 345 Furthermore, it has been recognised that heavy metal treatment can induce global
27
28 346 biomolecular changes in lipids and proteins, implying exotic exposure may lead to the
29
30 347 development of relevant metabolic changes in cellular components, particularly the
31
32 348 membrane⁶¹⁻⁶³. A recent study, for instance, reported that Ag exposure could increase cellular
33
34 349 lipid contents while decrease membrane fluidity⁶¹, and the possible mechanism is upregulated
35
36 350 lipid biosynthesis, which is known to be associated with the reduced membrane permeability.

35 351 Besides bacterial type, exposure time and exposure category, nutrient depletion is also
36
37 352 found to be an influential factor in the bacterial antimicrobial response. Here, bacterial cells
38
39 353 tend to adapt to new environmental stimuli after entering into a long-term nutrient-deprived
40
41 354 situation. From the cluster vectors analysis (Figure 1), spectral alterations in both strains from
42
43 355 Day 6 show slight peak shifts, which can be regarded as a potential signal showing that
44
45 356 bacterial cells are undergoing adaption. Additionally, *M. vanbaalenii* becomes a persistent
46
47 357 suspension in the media on entering a dormant state from Day 6. This is because bacteria in a
48
49 358 non-growing state can survive for much longer time under conditions of reduced oxygen or
50
51 359 nutrient deprivation^{46, 47}. Upon starvation, bacterial cells fragment into small spheroids
52
53 360 exhibiting rapid and drastic decreases in endogenous metabolism. This reorganization gives
54
55 361 bacteria maximum survival during long-term starvation. Specifically, bacteria on starvation
56
57 362 initially induce dwarfing generating cell number increases *via* fragmentation over the first 1
58
59 363 to 2 h and continuous size reductions in the fragmented cells, but no further increase in
60
364 numbers. After dwarfing phases, cell size continues to get smaller, with little or no metabolic
365 activity, and slow loss of viability⁶⁴. It has been reported that non-growing phase bacteria

1
2
3 366 adapt to and increase their tolerance to environmental stresses and such developed persistent
4
5 367 bacilli are capable of surviving several months of combinatorial antibiotic treatment⁴⁷, which
6
7 368 implies that stressed living conditions, to some extent and paradoxically, could help microbial
8
9 369 resistance to antimicrobial effects.

10 370 **4. Conclusions**

11
12
13 371 In the present study, we employed spectrochemical analysis coupled with multivariate
14
15 372 analysis as a robust tool towards investigating bacterial responses to long-term and low-level
16
17 373 exposure of antimicrobials under nutrient depletion conditions. ATR-FTIR spectroscopy
18
19 374 shows feasibility in revealing sufficient biochemical information continuously even at
20
21 375 extremely low-level exposures in a starvation situation, which fits better with real-world
22
23 376 circumstances and the natural state of microcosms. From the multivariate analysis of spectra
24
25 377 coupled with MRT, we evaluate the significance of different factors on long-term bacterial
26
27 378 responses to antimicrobials and find pivotal roles for exposure time and nutrient depletion.
28
29 379 Nutrient depletion can drive bacterial cells to either enter into a dormant state or exhibit
30
31 380 extra-cellular components against environmental antimicrobials, consequently causing a
32
33 381 broader range of spectral alteration compared to short-term exposures. Differences in
34
35 382 bacterial behaviours towards antimicrobials are also found between bacterial types (Gram-
36
37 383 positive *versus* Gram-negative) attributed to variations in cell wall structure. Our work is the
38
39 384 first revealing of the more important roles of exposure duration and nutrient depletion, rather
40
41 385 than of antimicrobial reagents, on microbial responses to low-level and prolonged
42
43 386 environmental exposures. We believe this approach has an important future with potential
44
45 387 feasibility in *in situ* screening of environmental exposures in real-time.

46 388 **Conflicts of interest**

47
48 389 There are no conflicts of interest to declare.

49 390 **Acknowledgement**

50 391 N.J. was funded by Chinese Academy of Sciences and China Scholarship Council.
51
52 392
53
54 393
55
56 394
57
58
59
60

395 **References**

- 396 1. J. Conly, *Can. Med. Assoc. J.*, 2002, **167**, 885-891.
- 397 2. J. W. Harrison and T. A. Svec, *Quintessence Int.*, 1998, **29**, 223-229.
- 398 3. J. C. Chee-Sanford, R. I. Aminov, I. J. Krapac, N. Garrigues-Jeanjean and R. I.
399 Mackie, *Appl. Environ. Microbiol.*, 2001, **67**, 1494-1502.
- 400 4. G. Hamscher, S. Sczesny, H. Hoper and H. Nau, *Anal Chem*, 2002, **74**, 1509-1518.
- 401 5. X. L. Ji, Q. H. Shen, F. Liu, J. Ma, G. Xu, Y. L. Wang and M. H. Wu, *J. Hazard*
402 *Mater.*, 2012, **235**, 178-185.
- 403 6. L. Cantas, S. Q. A. Shah, L. M. Cavaco, C. M. Manaia, F. Walsh, M. Popowska, H.
404 Garelick, H. Burgmann and H. Sorum, *Front. Microbiol.*, 2013, **4**, 14.
- 405 7. A. Koluman and A. Dikici, *Crit. Rev. Microbiol.*, 2013, **39**, 57-69.
- 406 8. M. Tandukar, S. Oh, U. Tezel, K. T. Konstantinidis and S. G. Pavlostathis, *Environ.*
407 *Sci. Technol.*, 2013, **47**, 9730-9738.
- 408 9. J. L. Martinez and F. Baquero, *Ups. J. Med. Sci.*, 2014, **119**, 68-77.
- 409 10. J. S. Kim, E. Kuk, K. N. Yu, J. H. Kim, S. J. Park, H. J. Lee, S. H. Kim, Y. K. Park,
410 Y. H. Park, C. Y. Hwang, Y. K. Kim, Y. S. Lee, D. H. Jeong and M. H. Cho,
411 *Nanomed.-Nanotechnol. Biol. Med.*, 2014, **10**, 1119-1119.
- 412 11. C. N. Lok, C. M. Ho, R. Chen, Q. Y. He, W. Y. Yu, H. Sun, P. K. H. Tam, J. F. Chiu
413 and C. M. Che, *J. Biol. Inorg. Chem.*, 2007, **12**, 527-534.
- 414 12. H. H. Lara, N. V. Ayala-Nunez, L. D. I. Turrent and C. R. Padilla, *World J.*
415 *Microbiol. Biotechnol.*, 2010, **26**, 615-621.
- 416 13. C. Marambio-Jones and E. M. V. Hoek, *J. Nanopart. Res.*, 2010, **12**, 1531-1551.
- 417 14. R. J. Griffitt, N. J. Brown-Peterson, D. A. Savin, C. S. Manning, I. Boube, R. A. Ryan
418 and M. Brouwer, *Environ. Toxicol. Chem.*, 2012, **31**, 160-167.
- 419 15. A. Gupta and S. Silver, *Nat. Biotechnol.*, 1998, **16**, 888-888.
- 420 16. N. F. Jin, D. Y. Zhang and F. L. Martin, *Integr. Biol.*, 2017, **9**, 406-417.
- 421 17. P. Marschner, C. H. Yang, R. Lieberei and D. E. Crowley, *Soil Biol Biochem*, 2001,
422 **33**, 1437-1445.
- 423 18. E. K. Costello, C. L. Lauber, M. Hamady, N. Fierer, J. I. Gordon and R. Knight,
424 *Science*, 2009, **326**, 1694-1697.
- 425 19. C. L. Lauber, M. Hamady, R. Knight and N. Fierer, *Appl. Environ. Microbiol.*, 2009,
426 **75**, 5111-5120.
- 427 20. M. Wietz, B. Wemheuer, H. Simon, H. A. Giebel, M. A. Seibt, R. Daniel, T.
428 Brinkhoff and M. Simon, *Environ. Microbiol.*, 2015, **17**, 3822-3831.
- 429 21. H. Li, F. L. Martin and D. Y. Zhang, *Anal. Chem.*, 2017, **89**, 3909-3918.
- 430 22. P. S. Stewart and J. W. Costerton, *Lancet*, 2001, **358**, 135-138.
- 431 23. N. Hoiby, T. Bjarnsholt, M. Givskov, S. Molin and O. Ciofu, *Int. J. Antimicrob.*
432 *Agents*, 2010, **35**, 322-332.
- 433 24. C. G. Mayhall and E. Apollo, *Antimicrob. Agents Chemother.*, 1980, **18**, 784-788.
- 434 25. M. R. W. Brown, D. G. Allison and P. Gilbert, *J. Antimicrob. Chemother.*, 1988, **22**,
435 777-780.
- 436 26. S. M. Ede, L. M. Hafner and P. M. Fredericks, *Appl. Spectrosc.*, 2004, **58**, 317-322.
- 437 27. O. I. Kalantzi, R. Hewitt, K. J. Ford, L. Cooper, R. E. Alcock, G. O. Thomas, J. A.
438 Morris, T. J. McMillan, K. C. Jones and F. L. Martin, *Carcinogenesis*, 2004, **25**, 613-
439 622.
- 440 28. J. L. Barber, M. J. Walsh, R. Hewitt, K. C. Jones and F. L. Martin, *Mutagenesis*,
441 2006, **21**, 351-360.
- 442 29. O. Fridman, A. Goldberg, I. Ronin, N. Shores and N. Q. Balaban, *Nature*, 2014, **513**,
443 418-421.

- 1
2
3 444 30. F. L. Martin, J. G. Kelly, V. Llabjani, P. L. Martin-Hirsch, Patel, II, J. Trevisan, N. J.
4 445 Fullwood and M. J. Walsh, *Nat. Protoc.*, 2010, **5**, 1748-1760.
5 446 31. M. J. Riding, F. L. Martin, J. Trevisan, V. Llabjani, Patel, II, K. C. Jones and K. T.
6 447 Semple, *Environ. Pollut.*, 2012, **163**, 226-234.
7 448 32. J. Li, R. Strong, J. Trevisan, S. W. Fogarty, N. J. Fullwood, K. C. Jones and F. L.
8 449 Martin, *Environ. Sci. Technol.*, 2013, **47**, 10005-10011.
9 450 33. M. J. Baker, J. Trevisan, P. Bassan, R. Bhargava, H. J. Butler, K. M. Dorling, P. R.
10 451 Fielden, S. W. Fogarty, N. J. Fullwood, K. A. Heys, C. Hughes, P. Lasch, P. L.
11 452 Martin-Hirsch, B. Obinaju, G. D. Sockalingum, J. Sule-Suso, R. J. Strong, M. J.
12 453 Walsh, B. R. Wood, P. Gardner and F. L. Martin, *Nat. Protoc.*, 2014, **9**, 1771-1791.
13 454 34. K. A. Heys, M. J. Riding, R. J. Strong, R. F. Shore, M. G. Pereira, K. C. Jones, K. T.
14 455 Semple and F. L. Martin, *Analyt.*, 2014, **139**, 896-905.
15 456 35. J. G. Kelly, J. Trevisan, A. D. Scott, P. L. Carmichael, H. M. Pollock, P. L. Martin-
16 457 Hirsch and F. L. Martin, *J. Proteome Res.*, 2011, **10**, 1437-1448.
17 458 36. J. Trevisan, P. P. Angelov, P. L. Carmichael, A. D. Scott and F. L. Martin, *Analyt.*,
18 459 2012, **137**, 3202-3215.
19 460 37. N. Jin, M. Paraskevaidi, K. T. Semple, F. L. Martin and D. Y. Zhang, *Anal Chem*,
20 461 2017, **89**, 9814-9821.
21 462 38. N. Jin, K. T. Semple, L. Jiang, C. Luo, D. Zhang and F. L. Martin, *Analyt.*, 2018, **143**,
22 463 768-776.
23 464 39. S. N. El Din, T. A. El-Tayeb, K. Abou-Aisha and M. El-Azizi, *Int. J. Nanomed.*,
24 465 2016, **11**, 1749-1758.
25 466 40. A. J. Kora and J. Arunachalam, *World J. Microbiol. Biotechnol.*, 2011, **27**, 1209-
26 467 1216.
27 468 41. J. T. H. Jo, F. S. L. Brinkman and R. E. W. Hancock, *Antimicrob. Agents Chemother.*,
28 469 2003, **47**, 1101-1111.
29 470 42. H. Wu, X. Shi, H. Wang and J. Liu, *J. Antimicrob. Chemother.*, 2000, **46**, 121-123.
30 471 43. J. Trevisan, P. P. Angelov, A. D. Scott, P. L. Carmichael and F. L. Martin,
31 472 *Bioinformatics*, 2013, **29**, 1095-1097.
32 473 44. F. L. Martin, M. J. German, E. Wit, T. Fearn, N. Ragavan and H. M. Pollock, *J.*
33 474 *Comput. Biol.*, 2007, **14**, 1176-1184.
34 475 45. J. Li, G. G. Ying, K. C. Jones and F. L. Martin, *Analyt.*, 2015, **140**, 2687-2695.
35 476 46. J. C. Betts, P. T. Lukey, L. C. Robb, R. A. McAdam and K. Duncan, *Mol. Microbiol.*,
36 477 2002, **43**, 717-731.
37 478 47. T. Hampshire, S. Soneji, J. Bacon, B. W. James, J. Hinds, K. Laing, R. A. Stabler, P.
38 479 D. Marsh and P. D. Butcher, *Tuberculosis*, 2004, **84**, 228-238.
39 480 48. Z. Movasaghi, S. Rehman and I. U. Rehman, *Appl. Spectrosc. Rev.*, 2008, **43**, 134-
40 481 179.
41 482 49. M. Drapal, P. R. Wheeler and P. D. Fraser, *Microbiology-(UK)*, 2016, **162**, 1456-
42 483 1467.
43 484 50. J. R. Morones, J. L. Elechiguerra, A. Camacho, K. Holt, J. B. Kouri, J. T. Ramirez
44 485 and M. J. Yacaman, *Nanotechnology*, 2005, **16**, 2346-2353.
45 486 51. D. Schnappinger and W. Hillen, *Arch. Microbiol.*, 1996, **165**, 359-369.
46 487 52. S. R. Connell, C. A. Trieber, G. P. Dinos, E. Einfeldt, D. E. Taylor and K. H.
47 488 Nierhaus, *Embo J.*, 2003, **22**, 945-953.
48 489 53. A. M. Fayaz, K. Balaji, M. Girilal, R. Yadav, P. T. Kalaichelvan and R. Venketesan,
49 490 *Nanomed.-Nanotechnol. Biol. Med.*, 2010, **6**, 103-109.
50 491 54. C. Jernberg, S. Lofmark, C. Edlund and J. K. Jansson, *Microbiology-(UK)*, 2010, **156**,
51 492 3216-3223.
52 493 55. M. Argast and C. F. Beck, *Antimicrob. Agents Chemother.*, 1984, **26**, 263-265.

- 1
2
3 494 56. R. W. Bundtzen, A. U. Gerber, D. L. Cohn and W. A. Craig, *Rev. Infect. Dis.*, 1981,
4 495 **3**, 28-37.
5 496 57. K. Fuursted, A. Hjort and L. Knudsen, *J. Antimicrob. Chemother.*, 1997, **40**, 221-226.
6 497 58. F. Pomati, A. G. Netting, D. Calamari and B. A. Neilan, *Aquat. Toxicol.*, 2004, **67**,
7 498 387-396.
8 499 59. S. B. Levy, *J. Antimicrob. Chemother.*, 2002, **49**, 25-30.
9 500 60. Z. M. Xiu, J. Ma and P. J. J. Alvarez, *Environ Sci Technol*, 2011, **45**, 9003-9008.
10 501 61. R. Gurbanov, S. N. Ozek, S. Tunçer, F. Severcan and A. G. Gozen, *J. Biophotonics*,
11 502 2017, Doi: 10.1002/jbio.201700252.
12 503 62. R. Gurbanov, N. Simsek Ozek, A. G. Gozen and F. Severcan, *Anal Chem*, 2015, **87**,
13 504 9653-9661.
14 505 63. M. Kardas, A. G. Gozen and F. Severcan, *Aquat Toxicol*, 2014, **155**, 15-23.
15 506 64. S. Kjelleberg, B. A. Humphrey and K. C. Marshall, *Appl. Environ. Microbiol.*, 1983,
16 507 **46**, 978-984.
17
18
19
20 508
21
22 509
23
24
25
26
27
28
29
30
31
32
33
34
35
36
37
38
39
40
41
42
43
44
45
46
47
48
49
50
51
52
53
54
55
56
57
58
59
60